BULLETIN OF BIOMATHEMATICS

Bulletin of Biomathematics, 2024, 2(2), 133–161

https://www.bulletinbiomath.org
ISSN Online: 2980-1869 / Open Access
https://doi.org/10.59292/bulletinbiomath.2024006

RESEARCH PAPER

A fractional-order model of COVID-19 and Malaria co-infection

Livinus Loko Iwa [1,*,‡], **Andrew Omame** [1,2,‡] **and Simeon Chioma Inyama** [1,‡]

[1]Department of Mathematics, Federal University of Technology, Owerri, Nigeria, [2]Abdus Salam School of Mathematical Sciences, Government College University, Lahore, Pakistan

* Corresponding Author
‡ iwa.livinus@gmail.com (Livinus Loko Iwa); andrew.omame@futo.edu.ng (Andrew Omame); scinyama2011@yahoo.com (Simeon Chioma Inyama)

Abstract

This paper explores the co-infection dynamics of coronavirus disease 2019 (COVID-19) and Malaria using Caputo-type fractional derivative to further understand the disease interactions and implement effective control strategies. We demonstrate the positivity and boundedness of the solution through Laplace transform techniques and establish the existence and uniqueness of the solution, showcasing model stability using fractional-order stability theory. Simulation experiments across varying fractional orders and disease classes offer insights into the co-infection dynamics. This is a new model and the findings underscore the potential impact of control measures on mitigating co-infection under endemic conditions. We conclude that infection with malaria does not guarantee immunity to COVID-19 and infection with COVID-19 as well does not guarantee immunity to malaria.

Keywords: COVID-19; Malaria; vaccination; co-infection; model-fitting; simulations

AMS 2020 Classification: 92D30; 92D25; 92C42; 34C60

1 Introduction

Malaria is one of the most deadly diseases in the world's history. It is caused by Plasmodium parasite [1] and transmitted to humans through the bites of infectious female Anopheles mosquitoes. First discovered in 1880 in a military hospital in Algiers, Algeria [2], malaria has caused millions of deaths in the past and still poses a great threat despite scientific investigations for hundreds of years [3]. Although some countries in the world have attained an indigenous malaria-free state in some particular years [4], most others still suffer the menace. In 2015, about 218 million malaria cases were recorded worldwide with 453,000 cases of death [5]. Also, in 2019, about 229 million cases of malaria with another estimated 409 thousand deaths were recorded in the world [6].

➤ **Received:** 22.09.2023 ➤ **Revised:** 16.05.2024 ➤ **Accepted:** 10.07.2024 ➤ **Published:** 31.10.2024

According to the 2020 World Malaria Report, Nigeria's malaria prevalence rate is at 303 per 1000 of its population [7]. The malaria prevalence rate is affected significantly by regions, rural-urban, and socio-economic differences [8]. In Nigeria for instance, the malaria prevalence rate ranges from 16 percent in the South-South and South-East regions to 34 percent in the North-West region and 2.4 times in rural population than in urban population as reported by United States Agency for International Development [9]. Also in socioeconomic groups, there is a seven times positive difference between children in lower and higher socio-economic groups.

The COVID-19 pandemic has recently joined the league of most common deadly diseases in the world. [10] described it as a positive-sense RNA virus that originated in the seafood market of live animals with its first case traced to the city of Wuhan, China [11] in December 2019. COVID-19 is highly contagious with three main routes; respiratory droplets, contact, and airborne [12]. Infected individuals become symptomatic in stages, although its complete clinical manifestation is still not clear as of the time of this research [13]. Symptoms include fever, dry cough, sore throat, loss of smell and fatigue but in acute cases, it can lead to severe shortness of breath, hypoxia, and death [12, 14]. Evidence suggests that older individuals and those with compromised immune systems (from pre-existing conditions) are more likely to develop severe forms of COVID-19 [15]. In 2020, there were about 2,804,796 confirmed cases of COVID-19 in the world and 193,710 confirmed deaths [16]. Also, a total of 585,086,861 confirmed cases worldwide with a total of 6,422,914 deaths as of August 11, 2022 [17].

Malaria and COVID-19 are two life-threatening diseases that concurrently distort normal human activities. Realizing the transmissible routes of COVID-19, the government placed restrictions in markets, worship centers, airports, viewing centers, and other social gatherings to help reduce unguided transmission of the disease. These unusual by-laws lasted for weeks and even months interrupted routine malaria prevention and control measures and treatments, and by extension increased new malaria cases and exacerbated untreated ones [18]. This suggests that COVID-19 has caused havoc on every aspect of human life ranging from social, health, economy, and education [19]. About 241 million malaria cases and 627 thousand deaths were recorded in 2020 worldwide as against the previous year, which makes about 14 million extra cases and 69 thousand extra deaths in the latter year [18]. Approximately two-thirds of these increased deaths (47,000) were caused by the unavailability of malaria prevention, diagnosis and treatment linked to COVID-19 disruptions [18]. Confirming the possible link between COVID-19 and Malaria [20] found different types of Malaria associated with COVID-19 and stated that the prevalence of Malaria among COVID-19 patients in Sudan is 32.4 percent.

Mathematical models have been so important in studying the behavioral pattern of infectious diseases [21–28]. The mathematical model of malaria transmission was first developed by Ross [26]. His report showed that reducing the vector population to below a certain threshold can help eradicate malaria. Chiyaka et al. [23] formulated a deterministic model with two latent periods in the non-constant host and vector populations. While checking for ways to eradicate the disease, they uniquely analyzed the spread of resistance and combined effects of intervention strategies such as personal protection, vaccination and treatment with the assumption that the treated individuals remain infectious for a while and discovered that personal control has a positive impact on disease control. To ascertain the level of awareness of COVID-19 virus [28] studied the mathematical model of COVID-19 which incorporates awareness programs and different hospitalization strategies for mild and severe cases while [29] proposed an SEIQCRW transmission model which adopts the SEIR model to study the current outbreak of COVID-19 in Nigeria with nonlinear forces on infection. While considering the complexity of the disease [19] formulated a stochastic model of COVID-19 under environmental white noise and recognized the random nature of the input components. Several other mathematical models on COVID-19 are found in

the literature, some of which are co-infection models [30–33].

Fractional differential equations have been widely used in recent years in modeling physical and biological processes [33–41]. This is mainly because of some level of limitations exhibited by mathematical models in integer-order derivatives. Although classical integer-order derivatives yield good results, fractional-order derivatives are non-local operators and produce better and more realistic results for a given real-life problem [41]. To further understand the different fractional order operators and models, see [42–46]. Caputo fractional derivative as one of the fractional differential operators is mostly used in modeling feasible real-life problems. This is because of its convenience for the initial condition of the fractional differential equations. It has long-term memory effects [21], and is very useful in translating higher fractional-order differential systems to lower ones [47] with well-understood physical meaning compared to other fractional operators [48]. [49] confirmed this when they analyzed the co-infection of HPV-CT in fractional order using Caputo fractional derivative. Also [50] compared Caputo, Caputo-Fabrizio and Atangana-Baleanu derivatives in their work. Their comparison shows that the Caputo derivative presents better results in the form of stability. Other mathematical models with fractional-order derivatives can be found in the works of [38, 51].

There are so many separate mathematical models in the literature on malaria and COVID-19 pandemic, however [27] started the work on the co-infection of the two diseases. They first derived the sufficient conditions for the stability of the two diseases separately before considering their entire equilibria where their findings suggest that using Malaria and COVID-19 protection measures concurrently is best compared to dealing with them separately. [52] studied the fractional-order mathematical model of COVID-19 and Malaria using the Atangana-Baleanu derivative and discovered they could reduce the risk factor of getting COVID-19 after contracting Malaria and vice versa. Still on the co-infection of COVID-19 and malaria [53] worked on the impact of COVID-19 and Malaria co-infection on clinical outcomes and discovered that patients with concurrent malaria and COVID-19 infection had greater mortality risk compared to mono-infection with Severe Acute Respiratory Syndrome Coronavirus 2 (SARS-CoV-2). Inspired by the above literature, especially the work performed by [27] and the beautiful patterns and results gotten from fractional derivatives as put together by [21, 41, 52, 54], we present this study of the co-infection of COVID-19 and malaria in fractional order derivative using Caputo fractional operator since the works of [27] and [53] are in integer derivative and [52] used Atangana-Baleanu fractional derivative. We expect to obtain better results considering the stated advantages.

The ensuing parts of this paper (in sections) are as follows: Section 2 captures the preliminaries where major definitions of the various fractional-order derivative operators are stated for easy and better understanding of the whole work. In Section 3, we formulated the fractional mathematical model and also carried out some vital analysis on the formulated model which included analysis on the invariant domain, positivity, basic reproduction number, locally asymptotic stability, existence and uniqueness of the solution and lastly the generalized Ulam-Hyers-Rassias stability. In Section 4 we performed some numerical simulations and discussed our results therein. Lastly, we concluded Section 5 based on our findings.

2 Preliminaries

This particular section presents some definitions of fractional derivatives and integrals that are of great relevance to modeling real-life problems.

Definition 1 *[55]: The Caputo fractional derivative of order $\omega > 0$ of a function $f(t)$ of order $\omega \in \mathbb{R}^+$ is given as*

$$ {}^{C}D_t^{\omega} f(t) = J_t^{n-\omega} D^n f(t) = \frac{1}{\Gamma(n-\omega)} \int_0^t (t-\tau)^{n-\omega-1} f^{(n)}(\tau) d\tau, \tag{1} $$

with the positive integer n given as $n-1 < \omega \leq n$. As $0 < \omega \leq 1$, the Caputo fractional derivative of order $\omega > 0$ above becomes

$$ {}^{C}D_t^{\omega} f(t) = \frac{1}{\Gamma(1-\omega)} \int_0^t (t-\tau)^{-\omega} f'(\tau) d\tau. \tag{2} $$

Definition 2 *[54]: Suppose that a function $f \in C^1(0, Y)$ is such that $T > 0$ and $0 < \omega \leq 1$, then Atangana-Baleanu derivative in Caputo sense is presented as*

$$ {}_{a}^{ABC}D_t^{\omega} f(t) = \frac{S(\omega)}{1-\omega} \int_a^t E_{\omega} \left(-\omega \frac{(t-\tau)^{\omega}}{1-\omega} \right) f'(\tau) d\tau, \quad t > 0, \tag{3} $$

where $S(\omega) = (1-\omega) + \frac{\omega}{\Gamma(\omega)}$, denotes a normalization function satisfying $S(0) = S(1) = 1$.

Definition 3 *[48]: The fractional integral of order $\omega > 0$ of any function $f \in C^1(0, Y)$ is presented as*

$$ J_t^{\omega} f(t) = \frac{1}{\Gamma(\omega)} \int_0^t (t-\tau)^{\omega-1} f(\tau) d\tau, \quad t > 0, \tag{4} $$

as long as the integral part is integrable in $\mathbb{R}^+$. In other words, suppose that $f(t) = P$, where P is a constant and results to;

$$ J_t^{\omega}(P) = \frac{1}{\Gamma(\omega)} \int_0^t (t-\tau)^{\omega-1} (P) d\tau = P \frac{t^{\omega}}{\Gamma(\omega+1)}. \tag{5} $$

Definition 4 *The solution of the Caputo fractional derivative can be written in the form of the Volterra integral as given below;*

$$ f - f(0) = \frac{1}{\Gamma(\omega)} \int_0^t (t-\tau)^{\omega-1} K(\tau, f(\tau)) d\tau, $$

where the fractional order $\omega > 0$.

Definition 5 *[55]: The Laplace transform of Caputo fractional derivative (2) is presented as;*

$$ \mathcal{L}\{D_t^{\omega} f(t)\} = s^{\omega} \tilde{f}(s) - s^{\omega-1} f(0), \quad 0 < \omega \leq 1, \tag{6} $$

with $\mathcal{L}$ as the Laplace transform operator.

3 Mathematical model formulation

The fractional-order model under this study is an interaction between human and vector populations. The human population at time t, denoted by $N_{\text{H}}(t)$ is sub-divided into seven distinct classes,

namely; susceptible humans $S_{H}(t)$, susceptible humans vaccinated against COVID-19 $V_{HC}(t)$, individuals infected with malaria $I_{HM}(t)$, recovered individuals from malaria $R_{HM}(t)$, individuals infected with COVID-19 $I_{HC}(t)$, recovered individuals from COVID-19 $R_{HC}(t)$ and individuals co-infected with malaria and COVID-19 $I_{MC}(t)$. Therefore,

$$N_{H}(t) = S_{H}(t) + V_{HC}(t) + I_{HM}(t) + R_{HM}(t) + I_{HC}(t) + R_{HC}(t) + I_{MC}(t).$$

We considered the last stage of the mosquito life cycle and sub-divided the vector population at time t, denoted by $N_{V}(t)$ into two distinct classes; susceptible vectors $S_{V}(t)$ and infectious vectors with malaria $I_{VM}(t)$ hence the vector population is given by

$$N_{V}(t) = S_{V}(t) + I_{VM}(t).$$

The model flow diagram is depicted in Figure 1 while the parameters of the model are described properly in Table 1 below.

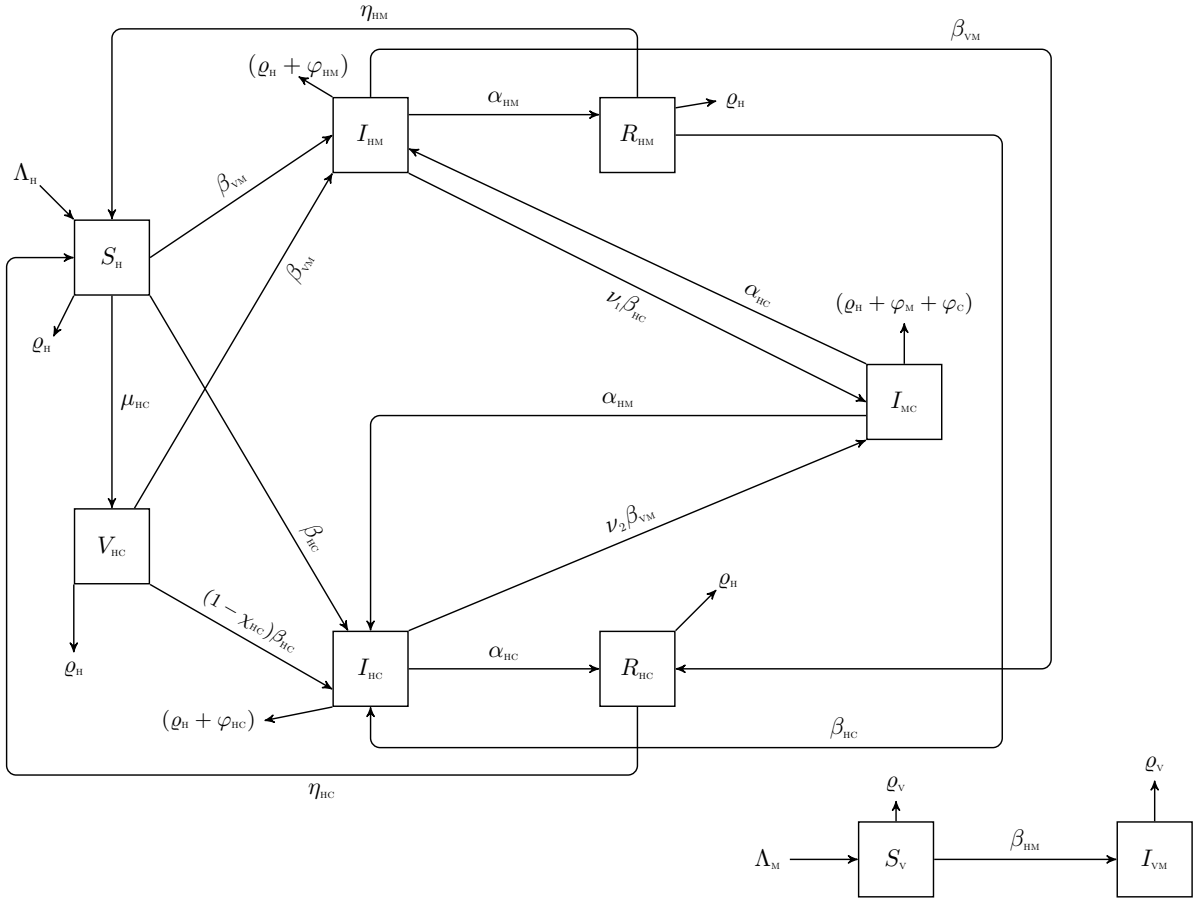

Figure 1. Model diagram

The rate of recruitment into the susceptible human population is given by Λ_{H} and that of the vector population is given by Λ_{V}. The parameter ϱ_{H} is the natural human mortality rate. It is assumed that infectious individuals can contact Malaria and/or COVID-19 individuals at the rates ϑ_{HM} and ϑ_{HC}, respectively. The interacting ability between the human and vector population warrants that individuals can move from one class to another. When treated, humans infected with Malaria move to the recovered class at the rate α_{HM}. Also, the human-to-unvaccinatedhuman transmission

Table 1. Description of variables and parameters in the above model equation

Variable	**Description**		
S_H	Susceptible humans		
V_{HC}	Susceptible humans vaccinated against COVID-19		
I_{HM}	Individuals infected with Malaria		
R_{HM}	Recovered individuals from Malaria		
I_{HC}	Individuals infected with COVID-19		
R_{HC}	Recovered individuals from COVID-19		
I_{MC}	Infectious individuals co-infected with Malaria and COVID-19		
S_V	Susceptible vectors		
I_{VM}	Infectious vectors with Malaria		
Parameter	Description	**Value**	**Reference**
Λ_H	Human recruitment rate	$\frac{206,139,587}{54.69\times365}day^{-}1$	[56, 57]
Λ_V	Vector recruitment rate	$\frac{10^4}{21}$	[56]
θ_2	Human contact rate with COVID-19 patients	0.4531	[58]
ϱ_H	Human natural death rate	$\frac{1}{54.69\times365}day^{-}1$	[56, 57]
η_{HM}	Loss of infection acquired immunity to Malaria	0.005	Assumed
η_{HC}	Loss of infection acquired immunity to COVID-19	0.005	Assumed
μ_{HC}	Fraction of susceptible humans vaccinated against COVID-19	0.025	[59]
χ_{HC}	COVID-19 vaccine efficacy	0.95	[14]
θ_1	Effective contact rate for vector to human transmission of Malaria	0.125 - 0.5	[60]
θ_3	Effective contact rate for human to vector transmission of Malaria	0.48	[61]
α_{HM}	Malaria recovery rate	0.25	[56]
α_{HC}	COVID-19 recovery rate	0.3	[62]
ϑ_1	Modification parameter accounting for susceptibility of Malaria-infected individuals to COVID-19	1	Assumed
ϑ_2	Modification parameter accounting for susceptibility of COVID-19-infected individuals to Malaria	1	Assumed
φ_{HM}	Malaria-induced death rate	0.000153	[7]
φ_{HC}	COVID-19-induced death rate	0.015	[63]
ϱ_V	Vector removal rate	$\frac{1}{21}$	[56, 57]

of COVID-19 is possible at the rate θ_2, especially when safety measures are neglected and the recovery rate of infected humans with COVID-19 is α_{HC}. χ_{HC} is the COVID-19 vaccine efficacy and θ_1 is the contact rate for vector to human transmission of Malaria. ϑ_1 is the modification parameter accounting for the susceptibility of Malaria-infected individuals to COVID-19 and ϑ_2 is the modification parameter accounting for susceptibility of COVID-19 infected individuals to Malaria. Mosquitoes are recruited into the population at the rate Λ_V and noting that the adult mosquito has a life span, we have the vector removal rate as ϱ_V.

Following the assumptions above, the COVID-19 and Malaria co-infection model is given by the following fractional differential equations;

$$
\begin{aligned}
{}^{C}D_t^{\omega}S_H(t) &= \Lambda_H - \left(\frac{\beta_{VM}I_{VM}}{N_H} + \frac{\beta_{HC}(I_{HC}+I_{MC})}{N_H}\right)S_H - \varrho_H S_H - \mu_{HC}S_H + \eta_{HM}R_{HM} + \eta_{HC}R_{HC},\\
{}^{C}D_t^{\omega}V_{HC}(t) &= \mu_{HC}S_H - (1-\chi_{HC})\frac{\beta_{HC}(I_{HC}+I_{MC})}{N_H}V_{HC} - \varrho_H V_{HC} - \frac{\beta_{VM}I_{VM}}{N_H}V_{HC},\\
{}^{C}D_t^{\omega}I_{HM}(t) &= \frac{\beta_{VM}I_{VM}}{N_H}(S_H + V_{HC} + R_{HC}) - (\alpha_{HM} + \varrho_H + \varphi_{HM})I_{HM} - \vartheta_1\frac{\beta_{HC}(I_{HC}+I_{MC})}{N_H}I_{HM} + \alpha_{HC}I_{MC},
\end{aligned}
$$

$$
\begin{aligned}
{}^{C}D_t^{\omega} R_{HM}(t) &= \alpha_{HM} I_{HM} - \varrho_H R_{HM} - \eta_{HM} R_{HM} - \frac{\beta_{HC}(I_{HC}+I_{MC})}{N_H} R_{HM},\\
{}^{C}D_t^{\omega} I_{HC}(t) &= \frac{\beta_{HC}(I_{HC}+I_{MC})}{N_H}(S_H + (1-\chi_{HC})V_{HC} + R_{HM}) - (\alpha_{HC}+\varrho_H+\varphi_{HC})I_{HC} - \vartheta_2 \frac{\beta_{VM} I_{VM}}{N_H} I_{HC} + \alpha_{HM} I_{MC},\\
{}^{C}D_t^{\omega} R_{HC}(t) &= \alpha_{HC} I_{HC} - \varrho_H R_{HC} - \eta_{HC} R_{HC} + \frac{\beta_{VM} I_{VM}}{N_H} R_{HC},\\
{}^{C}D_t^{\omega} I_{MC}(t) &= \vartheta_1 \frac{\beta_{HC}(I_{HC}+I_{MC})}{N_H} I_{HM} + \vartheta_2 \frac{\beta_{VM} I_{VM}}{N_H} I_{HC} - (\varrho_H + \varphi_{HM} + \varphi_{HC} + \alpha_{HM} + \alpha_{HC}) I_{MC},\\
{}^{C}D_t^{\omega} S_V(t) &= \Lambda_M - \frac{\beta_{HM}(I_{HM}+I_{MC})}{N_H} S_V - \varrho_V S_V,\\
{}^{C}D_t^{\omega} I_{VM}(t) &= \frac{\beta_{HM}(I_{HM}+I_{MC})}{N_H} S_V - \varrho_V I_{VM},
\end{aligned}
$$

with the corresponding initial conditions $S_H \geq (0)$, $V_{HC} \geq (0)$, $I_{HM} \geq (0)$, $R_{HM} \geq (0)$, $I_{HC} \geq (0)$, $R_{HC} \geq (0)$, $I_{MC} \geq (0)$, $S_V \geq (0)$, $I_{VM} \geq (0)$.

Invariant domain

Theorem 1 *Suppose $S_H(t), V_{HC}(t), I_{HM}(t), R_{HM}(t), I_{HC}(t), R_{HC}(t), I_{MC}(t)$ are solutions of the system of equations for the human population, then the set*

$$
\begin{aligned}
\Delta_h = \Big\{ &(S_H(t), V_{HC}(t), I_{HM}(t), R_{HM}(t), I_{HC}(t), R_{HC}(t), I_{MC}(t)) \in \mathbb{R}_+^7 : S_H \\
&+ V_{HC} + I_{HM} + R_{HM} + I_{HC} + R_{HC} + I_{MC} \leq \frac{\Lambda_H}{\varrho_H} \Big\},
\end{aligned} \tag{7}
$$

is positively invariant with respect to the model concerned.
For the vector population, Suppose $S_v(t), I_{VM}(t)$ are any solution of the system, then the set

$$
\Delta_v = \left\{ (S_V(t), I_{VM}(t)) \in \mathbb{R}_+^2 : S_V + I_{VM} \leq \frac{\Lambda_V}{\varrho_V} \right\}, \tag{8}
$$

is positively invariant with respect to the model concerned.

Proof We shall adopt the proof put together by [64].

Positivity

Following the pattern in the work of [48], by contradiction, we assume that equation three of the model is false. Then let $t_1 = \min\{t : S_H(t)V_{HM}(t)I_{HM}(t)R_{HM}(t)I_{HC}(t)R_{HC}(t)I_{MC}(t)\ S_v(t)I_{VM}(t) = 0\}$. Suppose $I_{HM}(t_1) = 0$, it implies that $S_H(t) > 0$, $V_{HC}(t) > 0$, $R_{HM}(t) > 0$, $I_{HC}(t) > 0$, $R_{HC}(t) > 0$, $I_{MC}(t) > 0$, $S_V(t) > 0$, $I_{VM}(t) > 0$ for all $[0, t_1]$. We can assume that there exists the following expression,

$$
\theta_1 = \min_{0 \leq t \leq t_t} \left\{ \frac{(\beta_{VM} I_{VM} S_H + \beta_{VM} I_{VM} R_{HC} + \beta_{VM} I_{VM} R_{HC} - \vartheta_1 \beta_{HC} I_{HC} - \vartheta_1 \beta_{HC} I_{MC})}{I_{HM}} - (\alpha_{HM} + \varrho_H + \varphi_{HM} + \alpha_{HC} I_{MC}) \right\}.
$$

It follows that

$$
{}^{C}D_t^{\omega} I_{HM} - \theta_1 I_{HM} > 0. \tag{9}
$$

We can also determine a continuous function Φ_1 to ascertain the following equation

$$^{C}D_t^{\omega} I_{\text{HM}} - \theta_1 I_{\text{HM}} = -\Phi_1(t).$$

By Laplace transform, the above inequality becomes

$$s^{\omega}\tilde{I}_{\text{HM}}(s) - s^{\omega-1} I_{\text{HM}}(0) - \theta_1 \tilde{I}_{\text{HM}}(s) = -\tilde{\Phi}_1(s),$$

from which

$$\begin{aligned} \tilde{I}_{\text{HM}}(s) &= I_{\text{HM}}(0)\frac{s^{\omega-1}}{s^{\omega}-\theta_1} - \frac{\Phi_1(s)}{s^{\omega}-\theta_1} \\ &= \frac{I_{\text{HM}}(0)}{s}\left(1-\frac{\theta_1}{s^{\omega}}\right)^{-1} - \frac{\Phi_1(s)}{s^{\omega}}\left(1-\frac{\theta_1}{s^{\omega}}\right)^{-1} \\ &= I_{\text{HM}}(0)\sum_{k=0}^{\infty}\frac{\theta_1^k}{s^{\omega k+1}} - \Phi_1(s)\sum_{k=0}^{\infty}\frac{\theta_1^k}{s^{\omega k+\omega}}. \end{aligned} \tag{10}$$

Ignoring the non-positive term, the inverse Laplace transform gives the solution of (9) (using Mittag-Leffler function), which satisfies the following expression:

$$I_{\text{HM}} > I_{\text{HM}}(0)\sum_{k=0}^{\infty}\frac{(\theta_1 t^{\omega})^k}{\Gamma(\omega k+1)} = I_{\text{HM}}(0)E_{\omega}\left(\theta_1 t^{\omega}\right),$$

such that the positivity of the solution I_{HM} is given by

$$I_{\text{HM}} > I_{\text{HM}}(0)E_{\omega}\left(\theta_1 t^{\omega}\right) > 0,$$

which contradicts $I_{\text{HM}}(t_1) = 0$. Similarly, suppose $I_{\text{MC}}(t_1) = 0$ which implies that $S_{\text{H}}(t) > 0$, $V_{\text{HC}}(t) > 0$, $R_{\text{HM}}(t) > 0$, $I_{\text{HM}}(t) > 0$, $R_{\text{HC}}(t) > 0$, $I_{\text{HC}}(t) > 0$, $S_{\text{V}}(t) > 0$, $I_{\text{VM}}(t) > 0$ for all $0 \le t \le t_1$. We assume that there exists the following expression:

$$\theta_2 = \min_{0\le t\le t_t}\left\{\frac{(\varphi_1\beta_{\text{HC}}I_{\text{HC}}I_{\text{HM}} + \varphi_1\beta_{\text{HC}}I_{\text{HM}} + \varphi_2\beta_{\text{VM}}I_{\text{VM}}I_{\text{HM}})}{I_{\text{MC}}} - (\varrho_{\text{H}} + \vartheta_{\text{M}} + \vartheta_{\text{C}} + \alpha_{\text{HM}} + \alpha_{\text{HC}})\right\},$$

so that

$$^{C}D_t^{\omega} I_{\text{MC}}(t) > \theta_2 I_{\text{MC}}(t). \tag{11}$$

We can still determine a continuous function $\Phi_2(t)$ to ascertain the following equation

$$^{C}D_t^{\omega} I_{\text{MC}}(t) - \theta_2 I_{\text{MC}}(t) = -\Phi_2(t).$$

By applying the Laplace transform, the above inequality becomes

$$s^{\omega}\tilde{I}_{\text{MC}}(s) - s^{\omega-1} I_{\text{MC}}(0) - \theta_2 \tilde{I}_{\text{MC}}(s) = -\tilde{\Phi}_2(s),$$

from which

$$\tilde{I}_{MC}(s) = I_c(0)\sum_{k=0}^{\infty}\frac{\theta_2^k}{s^{\omega k+1}} - \Phi_2(s)\sum_{k=0}^{\infty}\frac{\theta_2^k}{s^{\omega k+\omega}}.$$

Ignoring the non-positive term, the inverse Laplace transform gives the solution of Eq. (11) (using Mittag-Leffler function), satisfying the following expression:

$$I_{MC}(t) > I_{MC}(0)\sum_{k=0}^{\infty}\frac{(\theta_2 t^{\omega})^k}{\Gamma(\omega k+1)} = I_{MC}(0)E_{\omega}\left(\theta_2 t^{\omega}\right). \tag{12}$$

Hence the positivity of this other solution I_{MC} is given by $I_{MC}(t) > I_{MC}(0)E_{\omega}\left(\theta_2 t^{\omega}\right) > 0$, which contradicts $I_{MC}(t_1) = 0$. More so, since the above have similar results, the same pattern will show that the positivity of the solutions S_H, V_{HC}, R_{HM}, R_{HC}, S_V and V_{HC} respectively are given by

$$\begin{aligned}
I_{HC}(t) &> I_{HC}(0)E_{\omega}\left(\theta_3 t^{\omega}\right) > 0,\\
S_H(t) &> S_H(0)E_{\omega}\left(\theta_4 t^{\omega}\right) > 0,\\
V_{HC}(t) &> V_{HC}(0)E_{\omega}\left(\theta_5 t^{\omega}\right) > 0,\\
R_{HM}(t) &> R_{HM}(0)E_{\omega}\left(\theta_6 t^{\omega}\right) > 0,\\
R_{HC}(t) &> R_{HC}(0)E_{\omega}\left(\theta_7 t^{\omega}\right) > 0,\\
S_V(t) &> S_V(0)E_{\omega}\left(\theta_8 t^{\omega}\right) > 0,\\
I_{VM}(t) &> I_{VM}(0)E_{\omega}\left(\theta_9 t^{\omega}\right) > 0.
\end{aligned}$$

Basic reproduction number of the mathematical model

The Malaria-COVID-19 co-infection model has a disease-free equilibrium (DFE) as given below. First, we set the right-hand side of the equations to zero to obtain

$$\begin{aligned}
\xi_0 &= (S_H^0, V_{HC}^0, I_{HM}^0, R_{HM}^0, I_{HC}^0, R_{HC}^0, I_{MC}^0, S_V^0, I_{VM}^0)\\
&= \left(\frac{\Lambda_H}{\varrho_H+\mu_{HC}}, \frac{\mu_{HC}S_H}{\varrho_H}, 0, 0, 0, 0, 0, \frac{\Lambda_H}{\varrho_V}, 0\right).
\end{aligned} \tag{13}$$

We apply the next-generation operator method to the model. Matrix F is of new infection and matrix V is the transfer of infection in and out of the disease classes. Thus, we have

$$F = \begin{pmatrix}
0 & 0 & 0 & \beta_{VM}\\
0 & \frac{\beta_{HC}Q_1}{N_H} & \frac{\beta_{HC}Q_1}{N_H} & 0\\
0 & 0 & 0 & 0\\
\frac{\beta_{HM}S_V}{N_H} & 0 & \frac{\beta_{HM}S_V}{N_H} & 0
\end{pmatrix}, \tag{14}$$

where $Q_1 = [S_H + (1-\chi_{HC})]V_{HC}$.

$$V = \begin{pmatrix}
k_1 & 0 & -\alpha_{HC} & 0\\
0 & k_2 & -\alpha_{HM} & 0\\
0 & 0 & k_3 & 0\\
0 & 0 & 0 & \varrho_V
\end{pmatrix}, \tag{15}$$

where $k_1 = \alpha_{HM} + \varrho_H + \varphi_{HM}$, $k_2 = \alpha_{HC} + \varrho_H + \varphi_{HC}$, $k_3 = \varrho_H + \varphi_M + \varphi_C + \alpha_{HM} + \alpha_{HC}$. The basic reproduction number of the Malaria-COVID-19 co-infection model, denoted by $\mathcal{R}_0$ as illustrated in [65], is presented as $\mathcal{R}_0 = \max\{\mathcal{R}_{0M}, \mathcal{R}_{0C}\}$ where $\mathcal{R}_{0M}$ and $\mathcal{R}_{0C}$ are respectively the Malaria and COVID-19 associated reproduction numbers, given by

$$\mathcal{R}_{0M} = \sqrt{\frac{\beta_{HM}\beta_{VM}S_V^*}{\varrho_V k_1 N_H^*}}, \quad \text{and} \quad \mathcal{R}_{0C} = \frac{\beta_{HC}[S_H^* + (1-\chi_{HC})V_{HC}^*]}{k_2 N_H^*}.$$

Local asymptotic stability of disease-free equilibrium (DFE) of the co-infection model

Theorem 2 *At Disease-Free Equilibrium (DFE), the mathematical model is locally asymptotically stable (LAS) if $\mathcal{R}_0 < 1$, and unstable if $\mathcal{R}_0 > 1$.*

Proof The local stability of the model is analyzed using the Jacobean square matrix of the whole system, evaluated at COVID-19-Malaria-free equilibrium, given by;

$$J = \begin{pmatrix}
-(\varrho_H + \mu_{HC}) & 0 & 0 & \eta_{HM} & \frac{\beta_{HC}S_H}{N_H} & \eta_{HC} & \frac{\beta_{HC}S_H}{N_H} & 0 & \frac{\beta_{VM}S_H}{N_H} \\
\mu_{HC} & \varrho_H & 0 & 0 & -\frac{(1-\chi_{HC})\beta_{HC}V_{HC}}{N_H} & 0 & -\frac{(1-\chi_{HC})\beta_{HC}V_{HC}}{N_H} & 0 & \frac{\beta_{VM}V_{HC}}{N_H} \\
0 & 0 & -k_1 & 0 & 0 & 0 & \alpha_{HC} & 0 & \frac{\beta_{VM}(S_H+V_{HC})}{N_H} \\
0 & 0 & \alpha_{HM} & -(\varrho_H + \eta_{HM}) & 0 & 0 & 0 & 0 & 0 \\
0 & 0 & 0 & 0 & H - k_2 & 0 & H + \alpha_{HM} & 0 & 0 \\
0 & 0 & 0 & 0 & \alpha_{HC} & -(\varrho_H + \eta_{HC}) & 0 & 0 & 0 \\
0 & 0 & 0 & 0 & 0 & 0 & -k_3 & 0 & 0 \\
0 & 0 & -\frac{\beta_{HM}S_V}{N_H} & 0 & 0 & 0 & -\frac{\beta_{HM}S_V}{N_H} & -\varrho_V & 0 \\
0 & 0 & \frac{\beta_{HM}S_V}{N_H} & 0 & 0 & 0 & \frac{\beta_{HM}S_V}{N_H} & 0 & -\varrho_V
\end{pmatrix}, \tag{16}$$

where $H = \frac{\beta_{HC}[S_H + (1-\chi_{HC})V_{HC}]}{N_H}$.

The first three eigenvalues are $\lambda_1 = -(\eta_{HC} + \varrho_H)$, $\lambda_2 = -\varrho_V$ (twice), while the remaining eigenvalues will as well satisfy the negativity requirement for stability (following the method of Routh-Hurwitz).

Epidemiologically, Theorem 2 implies that the prevalence of COVID-19 and Malaria can be eradicated from the population when $\mathcal{R}_0$ and if the initial population of the model is in the region of attraction of the DFE. Hence, the DFE is locally asymptotically stable if $\mathcal{R}_0 = max(\mathcal{R}_{0C}, \mathcal{R}_{0M}) < 1$.

Existence and uniqueness of solution of the model

As significantly demonstrated by [66], we show the existence and uniqueness of the solution of the fractional-order model. When we apply the fractional integral to the Caputo fractional derivative model of order $\omega > 0$ while maintaining its initial conditions, we have the following Volterra-integral equations as a solution to the fractional model. This theory validates our claim that a solution to our model equations exists and is unique:

$$\begin{aligned}
S_H - S_H(0) &= \frac{1}{\Gamma(\omega)}\int_0^t (t-\tau)^{\omega-1} K(\tau, S_H(\tau))\, d\tau, \\
V_{HC} - V_{HC}(0) &= \frac{1}{\Gamma(\omega)}\int_0^t (t-\tau)^{\omega-1} Q(\tau, V_{HM}(\tau))\, d\tau, \\
I_{HM} - I_{HM}(0) &= \frac{1}{\Gamma(\omega)}\int_0^t (t-\tau)^{\omega-1} V(\tau, I_{HM}(\tau))\, d\tau,
\end{aligned} \tag{17}$$

$$
\begin{aligned}
R_{HM}(t) - R_{HM}(0) &= \frac{1}{\Gamma(\omega)} \int_0^t (t-\tau)^{\omega-1} F\left(\tau, R_{HM}(\tau)\right) d\tau, \\
I_{HC}(t) - I_{HC}(0) &= \frac{1}{\Gamma(\omega)} \int_0^t (t-\tau)^{\omega-1} H\left(\tau, I_{HC}(\tau)\right) d\tau, \\
R_{HC}(t) - R_{HC}(0) &= \frac{1}{\Gamma(\omega)} \int_0^t (t-\tau)^{\omega-1} G\left(\tau, R_{HC}(\tau)\right) d\tau, \\
I_{MC}(t) - I_{MC}(0) + &= \frac{1}{\Gamma(\omega)} \int_0^t (t-\tau)^{\omega-1} U\left(\tau, I_{MC}(\tau)\right) d\tau, \\
S_v(t) - S_v(0) &= \frac{1}{\Gamma(\omega)} \int_0^t (t-\tau)^{\omega-1} P\left(\tau, S_v(\tau)\right) d\tau, \\
I_{VM}(t) - I_{VM}(0) &= \frac{1}{\Gamma(\omega)} \int_0^t (t-\tau)^{\omega-1} W\left(\tau, I_{VM}(\tau)\right) d\tau.
\end{aligned}
$$

We assume that the functions $(K, Q, V, F, H, G, U, P, W) : [0, b] \times \mathbb{R} \to \mathbb{R}$ are continuous so that $(\mathbb{R}, \|.\|)$ is the Banach space and $\mathbb{H}^1([0, b])$ is that of all the continuous function defined in $[0, b] \to \mathbb{R}$ carved with Chebychev norm. We now prove that the continuous functions K, Q, V, F, H, G, U, P and W satisfy the Lipschitz condition when

$$
\sup_{0<t\leq Y} \left\| \frac{I_{HM}}{N_H} \right\| \leq \Theta_1, \quad \sup_{0<t\leq Y} \left\| \frac{I_{HC}}{N_H} \right\| \leq \Theta_2, \quad \sup_{0<t\leq Y} \left\| \frac{I_{MC}}{N_H} \right\| \leq \Theta_3, \quad \sup_{0<t\leq Y} \left\| \frac{I_{VM}}{N_H} \right\| \leq \Theta_4.
$$

Thus, firstly we have

$$
\begin{aligned}
\|K(S_{H1}) - K(S_{H2})\| &= \left\| \Lambda_H - \left(\frac{\beta_{VM} I_{VM}}{N_H} + \frac{\beta_{HC}(I_{HC} + I_{MC})}{N_H} + \varrho_H + \mu_{HC} - \eta_{HM} R_{HM} - \eta_{HC} R_{HC} \right) S_{H1} \right. \\
&- \left. \left(\Lambda_H - \left(\frac{\beta_{VM} I_{VM}}{N_H} + \frac{\beta_{HC}(I_{HC} + I_{MC})}{N_H} + \varrho_H + \mu_{HC} - \eta_{HM} R_{HM} - \eta_{HC} R_{HC} \right) S_{H2} \right) \right\| \\
&= \left\| -\frac{\beta_{VM} I_{VM}}{N_H} (S_{H1} - S_{H2}) - \frac{\beta_{HC} I_{HC}}{N_H} (S_{H1} - S_{H2}) - \frac{\beta_{HC} I_{MC}}{N_H} (S_{H1} - S_{H2}) - \varrho_H (S_{H1} - S_{H2}) \right. \\
&- \left. \mu_{HC} (S_{H1} - S_{H2}) + \eta_{HM} R_{HM} (S_{H1} - S_{H2}) + \eta_{HC} R_{HC} (S_{H1} - S_{H2}) \right\| \\
&\leq \beta_{VM} \sup_{0\leq t\leq Y} \left\| \frac{I_{VM}}{N_H} \right\| \|S_{H1} - S_{H2}\| + \beta_{HC} \sup_{0\leq t\leq Y} \left\| \frac{I_{HC}}{N_H} \right\| \|S_{H1} - S_{H2}\| \\
&+ \beta_{HC} \sup_{0\leq t\leq Y} \left\| \frac{I_{MC}}{N_H} \right\| \|S_{H1} - S_{H2}\| + \varrho_H \|S_{H1} - S_{H2}\| + \mu_{HC} \|S_{H1} - S_{H2}\| \\
&+ \eta_{HM} R_{HM} \|S_{H1} - S_{H2}\| + \eta_{HC} R_{HC} \|S_{H1} - S_{H2}\| \\
&\leq L_K \|S_{H1} - S_{H2}\|, \qquad (18)
\end{aligned}
$$

where

$$
L_K = \beta_{VM}\Theta_4 + \beta_{HC}\Theta_2 + \beta_{HC}\Theta_3 + \varrho_H + \mu_{HC} + \eta_{HM} R_{HM} + \eta_{HC} R_{HC} > 0.
$$

Secondly,

$$
\|Q(V_{HC1}) - Q(V_{HC2})\| = \left\| \mu_{HC} S_H - \left(\frac{\beta_{HC} I_{HC}}{N_H} + \frac{\chi_{HC} I_{MC}}{N_H} - \varrho_H - \frac{\beta_{VM} I_{VM}}{N_H} \right) V_{HC1} \right.
$$

$$
\begin{aligned}
- & \left(\mu_{HC} S_H - \left(\frac{\beta_{HC} I_{HC}}{N_H} + \frac{\chi_{HC} I_{MC}}{N_H} - \varrho_H - \frac{\beta_{VM} I_{VM}}{N_H}\right) V_{HC2}\right)\Bigg\| \\
= & -\left(\frac{\beta_{HC} I_{HC}}{N_H} + \frac{\chi_{HC} I_{MC}}{N_H} - \varrho_H - \frac{\beta_{VM} I_{VM}}{N_H}\right) \|V_{HC1} - V_{HC2}\| \\
\leq & \left(\beta_{HC} \sup_{0\leq t\leq Y} \left\|\frac{I_{HC}}{N_H}\right\| + \chi_{HC} \sup_{0\leq t\leq Y} \left\|\frac{I_{MC}}{N_H}\right\| + \beta_{VM} \sup_{0\leq t\leq Y} \left\|\frac{I_{VM}}{N_H}\right\| + \varrho_H\right) \|V_{HC1} - V_{HC2}\| \\
\leq & L_Q \|V_{HC1} - V_{HC2}\|,
\end{aligned} \tag{19}
$$

where

$$L_Q = \beta_{HC}\Theta_2 + \chi_{HC}\Theta_3 + \beta_{VM}\Theta_4 + \varrho_H > 0.$$

Applying a similar approach gives the following

$$
\begin{aligned}
\|V(I_{HM1}) - V(I_{HM2})\| = & \left\|\frac{\beta_{VM} I_{VM} S_H}{N_H} + \frac{\beta_{VM} I_{VM} V_{HC}}{N_H} + \frac{\beta_{VM} I_{VM} R_{HC}}{N_H} - \left(\alpha_{HM} + \varrho_H + \varphi_{HM} + \frac{\vartheta_1 B_{HC} I_{HC}}{N_H} + \frac{\vartheta_1 I_{MC}}{N_H} - \alpha_{HM}\right) I_{HM1}\right\| \\
- & \left\|\frac{\beta_{VM} I_{VM} S_H}{N_H} + \frac{\beta_{VM} I_{VM} V_{HC}}{N_H} + \frac{\beta_{VM} I_{VM} R_{HC}}{N_H} - \left(\alpha_{HM} + \varrho_H + \varphi_{HM} + \frac{\vartheta_1 B_{HC} I_{HC}}{N_H} + \frac{\vartheta_1 I_{MC}}{N_H} - \alpha_{HM}\right) I_{HM2}\right\| \\
= & \left(\alpha_{HM} + \varrho_H + \varphi_{HM} + \left(\frac{\vartheta_1 B_{HC} I_{HC}}{N_H} + \frac{\vartheta_1 I_{MC}}{N_H}\right)\right) \|I_{HM1} - I_{HM2}\| \\
\leq & L_V \|I_{HM1} - I_{HM2}\|,
\end{aligned} \tag{20}
$$

where

$$L_V = \vartheta_1 B_{HC}\Theta_2 + \vartheta_1\Theta_3 + \alpha_{HM} + \varrho_H + \varphi_{HM} > 0.$$

$$
\begin{aligned}
\|F(R_{HM1}) - F(R_{HM2})\| = & \left\|\alpha_{HM} I_{HM} - \varrho_H - \eta_{HM} - \left(\frac{\beta_{HC} I_{HC}}{N_H} - \frac{\beta_{HC} I_{MC}}{N_H}\right) R_{HM1}\right. \\
- & \left.\left(\alpha_{HM} I_{HM} - \varrho_H - \eta_{HM} - \left(\frac{\beta_{HC} I_{HC}}{N_H} - \frac{\beta_{HC} I_{MC}}{N_H}\right) R_{HM2}\right)\right\| \\
\leq & L_F \|R_{HM1} - R_{HM2}\|,
\end{aligned} \tag{21}
$$

where

$$L_F = \beta_{HC}\Theta_2 + \beta_{HC}\Theta_3 > 0.$$

$$
\begin{aligned}
\|H(I_{HC1}) - H(I_{HC2})\| = & \left\|\left(\frac{\beta_{HC} S_H}{N_H} + \frac{\beta_{HC} I_{MC} S_H}{N_H} + \frac{\beta_{HC} V_{HC}}{N_H} + \frac{\beta_{HC} I_{MC} V_{HC}}{N_H} - \frac{\beta_{HC}\chi_{HC} V_{HC}}{N_H} - \frac{\beta_{HC} I_{MC}\chi_{HC} V_{HC}}{N_H}\right.\right. \\
+ & \left.\frac{\beta_{HC} R_{HC}}{N_H} + \frac{\beta_{HC} I_{MC} R_{HC}}{N_H} - \alpha_{HC} - \varrho_H + \varphi_{HC} - \frac{\vartheta_2 \beta_{VM} I_{VM}}{N_H} + \alpha_{HM} I_{MC}\right) I_{HC1} \\
- & \left(\frac{\beta_{HC} S_H}{N_H} + \frac{\beta_{HC} I_{MC} S_H}{N_H} + \frac{\beta_{HC} V_{HC}}{N_H} + \frac{\beta_{HC} I_{MC} V_{HC}}{N_H} - \frac{\beta_{HC}\chi_{HC} V_{HC}}{N_H} - \frac{\beta_{HC} I_{MC}\chi_{HC} V_{HC}}{N_H}\right. \\
+ & \left.\left.\frac{\beta_{HC} R_{HC}}{N_H} + \frac{\beta_{HC} I_{MC} R_{HC}}{N_H} - \alpha_{HC} - \varrho_H + \varphi_{HC} - \frac{\vartheta_2 \beta_{VM} I_{VM}}{N_H} + \alpha_{HM} I_{MC}\right) I_{HC2}\right\| \\
\leq & L_H \|I_{HC1} - I_{HC2}\|,
\end{aligned} \tag{22}
$$

where

$$L_{\text{H}} = \beta_{\text{HC}}\chi_{\text{HC}}\Theta_1 + \beta_{\text{HC}}\chi_{\text{HC}}\Theta_2 + \vartheta_2\beta_{\text{VM}}\Theta_4 + \alpha_{\text{HC}} + \varrho_{\text{H}} > 0.$$

$$\begin{aligned} \|G(R_{\text{HC1}}) - G(R_{\text{HC2}})\| &= \left\| \left(\alpha_{\text{HC}} I_{\text{HC}} - \varrho_{\text{H}} - \eta_{\text{HC}} - \frac{\beta_{\text{VM}} I_{\text{VM}}}{N_{\text{H}}} \right) R_{\text{HC1}} \right. \\ &- \left. \left(\alpha_{\text{HC}} I_{\text{HC}} - \varrho_{\text{H}} - \eta_{\text{HC}} - \frac{\beta_{\text{VM}} I_{\text{VM}}}{N_{\text{H}}} \right) R_{\text{HC2}} \right\| \\ &\leq L_{\text{G}} \left\| R_{\text{HC1}} - R_{\text{HC2}} \right\|, \end{aligned} \tag{23}$$

where

$$L_{\text{G}} = \beta_{\text{VM}}\Theta_4 + \varrho_{\text{H}} + \eta_{\text{HC}} > 0.$$

$$\begin{aligned} \|U(I_{\text{MC1}}) - U(I_{\text{MC2}})\| &= \left\| \left(\frac{\vartheta_1\beta_{\text{HC}} I_{\text{HC}}\mathfrak{I}_{\text{HM}}}{N_{\text{H}}} + \frac{\vartheta_1\beta_{\text{HC}} I_{\text{HM}}}{N_{\text{H}}} + \frac{\vartheta_2\beta_{\text{VM}} I_{\text{VM}} I_{\text{HM}}}{N_{\text{H}}} - \varrho_{\text{H}} - \varphi_{\text{M}} - \varphi_{\text{C}} - \alpha_{\text{HM}} - \alpha_{\text{HC}} \right) I_{\text{MC1}} \right. \\ &- \left. \left(\frac{\vartheta_1\beta_{\text{HC}} I_{\text{HC}}\mathfrak{I}_{\text{HM}}}{N_{\text{H}}} + \frac{\vartheta_1\beta_{\text{HC}} I_{\text{HM}}}{N_{\text{H}}} + \frac{\vartheta_2\beta_{\text{VM}} I_{\text{VM}} I_{\text{HM}}}{N_{\text{H}}} - \varrho_{\text{H}} - \varphi_{\text{M}} - \varphi_{\text{C}} - \alpha_{\text{HM}} - \alpha_{\text{HC}} \right) I_{\text{MC2}} \right\| \\ &\leq L_{\text{U}} \left\| I_{\text{MC1}} - I_{\text{MC2}} \right\|, \end{aligned} \tag{24}$$

where

$$L_{\text{U}} = \varrho_{\text{H}} + \varphi_{\text{M}} + \varphi_{\text{C}} + \alpha_{\text{HM}} + \alpha_{\text{HC}} > 0.$$

$$\begin{aligned} \|P(S_{\text{V1}}) - P(S_{\text{V2}})\| &= \left\| \left(\Lambda_{\text{M}} - \frac{\beta_{\text{HM}} I_{\text{HM}}}{N_{\text{H}}} - \frac{\beta_{\text{HM}} I_{\text{MC}}}{N_{\text{H}}} - \varrho_{\text{V}} \right) S_{\text{V1}} - \left(\Lambda_{\text{M}} - \frac{\beta_{\text{HM}} I_{\text{HM}}}{N_{\text{H}}} - \frac{\beta_{\text{HM}} I_{\text{MC}}}{N_{\text{H}}} - \varrho_{\text{V}} \right) S_{\text{V2}} \right\| \\ &\leq L_{\text{P}} \left\| S_{\text{V1}} - S_{\text{V2}} \right\|, \end{aligned} \tag{25}$$

where

$$L_{\text{P}} = \beta_{\text{HM}}\Theta_1 + \beta_{\text{HM}}\Theta_2 + \varrho_{\text{V}} > 0.$$

$$\begin{aligned} \|W(I_{\text{VM1}}) - W(I_{\text{VM2}})\| &= \left\| \left(\frac{\beta_{\text{HM}} I_{\text{HM}} S_{\text{VM}}}{N_{\text{H}}} + \frac{\beta_{\text{HM}} I_{\text{MC}} S_{\text{VM}}}{N_{\text{H}}} - \varrho_{\text{V}} I_{\text{VM}} \right) I_{\text{VM1}} - \left(\frac{\beta_{\text{HM}} I_{\text{HM}} S_{\text{VM}}}{N_{\text{H}}} + \frac{\beta_{\text{HM}} I_{\text{MC}} S_{\text{VM}}}{N_{\text{H}}} - \varrho_{\text{V}} I_{\text{VM}} \right) I_{\text{VM2}} \right\| \\ &\leq L_{\text{W}} \left\| I_{\text{VM1}} - I_{\text{VM2}} \right\|, \end{aligned} \tag{26}$$

where

$$L_{\text{W}} = \varrho_{\text{V}} > 0.$$

Theorem 3 *Suppose* $\left(L_K, L_Q, L_V, L_F, L_H, L_G, L_U, L_P, L_W\right) \frac{\Gamma(1-\omega)\sin(\pi\omega)Y^{\omega}}{\omega\pi} < 1$, *we then say that the fractional model has a unique solution on the interval* $[0, b]$, *letting* $(K, Q, V, F, H, G, U, P, W) : [0, b] \times$

$\mathbb{R} \to \mathbb{R}$ *be continuous and satisfying the Lipschitz condition.*

Proof We can see the proof in the work of [67–69].

Furthermore, we look at the existence of solutions of the fractional model using Schaefer's fixed point theorem.

Theorem 4 *Suppose that* $(K, Q, V, F, H, G, U, P, W) : [0, b] \times \mathbb{R} \to \mathbb{R}$ *are continuous and that there exists constants* $(L_{K1}, L_{Q1}, L_{V1}, L_{F1}, L_{H1}, L_{G1}, L_{U1}, L_{P1}, L_{W1}) > 0$ *such that*

$$\|K(t, S_{H})\| \leq L_{K1}\left(g + \|S_{H}\|\right), \ \ \|Q(t, V_{HC})\| \leq L_{Q1}\left(g + \|V_{HC}\|\right), \ \ \|V(t, I_{HM})\| \leq L_{V1}\left(g + \|I_{HM}\|\right),$$

$$\|F(t, R_{HM})\| \leq L_{F1}\left(g + \|R_{HM}\|\right), \ \ \|H(t, I_{HC})\| \leq L_{H1}\left(g + \|I_{HC}\|\right), \ \ \|G(t, R_{HC})\| \leq L_{G1}\left(g + \|R_{HC}\|\right),$$

$$\|U(t, I_{MC})\| \leq L_{U1}\left(g + \|I_{MC}\|\right), \ \ \|P(t, S_{V})\| \leq L_{P1}\left(g + \|S_{V}\|\right), \ \ \|W(t, I_{VM})\| \leq L_{W1}\left(g + \|I_{VM}\|\right),$$

where $0 < g \leq 1$ *is an arbitrary number, then the system has at least one solution.*

Proof The proof of this result is similar to the approach used in ([67–69], and therefore omitted.

Generalized Ulam-Hyers-Rassias stability

This particular stability for fractional systems has been studied in a few literature. In this section we will adopt a similar approach in [70] to show that our fractional model is generalized Ulam-Hyers-Rassias (UHR) stable. Following [70], we have the definition below.

Definition 6 *The fractional model above is generalized UHR stable with respect to* $\Omega(t) \in \mathbb{H}^1([0, b], \mathbb{R})$ *if there exists a real value* $\kappa_\psi > 0$ *such that* $\epsilon > 0$ *and for every solution* $(S_{H}, V_{HM}, I_{HM}, R_{HM}, I_{HC}, R_{HC}, I_{MC}, S_{V}, I_{VM}) \in \mathbb{H}^1([0, b], \mathbb{R})$ *of the following inequalities*

$$\left|D_t^{\psi} S_{H}(t) - K(t, S_{H})\right| \leq \Omega(t), \ \ \left|D_t^{\psi} V_{HM} - Q(t, V_{HM})\right| \leq \Omega(t), \ \ \left|D_t^{\psi} I_{HM} - V(t, I_{HM})\right| \leq \Omega(t),$$

$$\left|D_t^{\psi} R_{HM}(t) - F(t, R_{HM}(t))\right| \leq \Omega(t), \ \ \left|D_t^{\psi} I_{HC}(t) - H(t, I_{HC}(t))\right| \leq \Omega(t), \ \ \left|D_t^{\psi} R_{HC}(t) - G(t, R_{HC}(t))\right| \leq \Omega(t),$$

$$\left|D_t^{\psi} I_{MC}(t) - U(t, I_{MC}(t))\right| \leq \Omega(t), \quad \left|D_t^{\psi} S_{V}(t) - P(t, S_{V}(t))\right| \leq \Omega(t),$$

$$\left|D_t^{\psi} I_{VM}(t) - W(t, I_{VM}(t))\right| \leq \Omega(t), \quad \left|D_t^{\psi} S_{V}(t) - P(t, S_{V}(t))\right| \leq \Omega(t),$$

there exists a solution $(\bar{S}_{H}, \bar{V}_{HM}, \bar{I}_{HM}, \bar{R}_{HM}, \bar{I}_{HC}, \bar{R}_{HC}, \bar{I}_{MC}, \bar{S}_{v}, \bar{I}_{VM}) \in \mathbb{H}^1([0, b], \mathbb{R})$ *of the fractional model with*

$$\left|S_{H}(t) - \bar{S}_{H}\right| \leq \kappa_\psi \Omega(t), \ \ \left|V_{HM} - \bar{V}_{HM}\right| \leq \kappa_\psi \Omega(t), \ \ \left|I_{HM} - \bar{I}_{HM}\right| \leq \kappa_\psi \Omega(t), \ \ \left|R_{HM}(t) - \bar{R}_{HM}(t)\right| \leq \kappa_\psi \Omega(t),$$

$$\left|I_{HC}(t) - \bar{I}_{HC}(t)\right| \leq \kappa_\psi \Omega(t), \ \ \left|R_{HC}(t) - \bar{R}_{HC}(t)\right| \leq \kappa_\psi \Omega(t), \ \ \left|I_{MC}(t) - \bar{I}_{MC}(t)\right| \leq \kappa_\psi \Omega(t),$$

$$\left|S_{\text{V}}(t)-\bar{S}_{\text{V}}(t)\right|\leq\kappa_{\psi}\Omega(t),\ \ \left|I_{\text{VM}}(t)-\bar{I}_{\text{VM}}(t)\right|\leq\kappa_{\psi}\Omega(t).$$

Theorem 5 *The fractional model is generalized Ulam-Hyers-Rassias stable with respect to* $\Omega\in\mathbb{H}^{1}([0,b],\mathbb{R})$ *if*

$$\left(L_{\text{K}},L_{\text{Q}},L_{\text{V}},L_{\text{F}},L_{\text{H}},L_{\text{G}},L_{\text{U}},L_{\text{P}},L_{\text{W}}\right)T^{\psi}<1.$$

Proof From Definition 6, let Ω denote the non-decreasing function of t, then there exists $\epsilon>0$ such that

$$\int_{0}^{t}(t-\tau)^{\psi-1}\Omega(\tau)d\tau\leq\epsilon\Omega(t),$$

for every $t\in[0,b]$. The functions K,Q,V,F,H,G,U,P,W have been shown to be continuous and

$$\left(L_{\text{K}},L_{\text{Q}},L_{\text{V}},L_{\text{F}},L_{\text{H}},L_{\text{G}},L_{\text{U}},L_{\text{P}},L_{\text{W}}\right)>0,$$

satisfies the Lipschitz condition as shown in the previous section. From Theorem 3, the fractional model has the unique solution

$$\bar{S}_{\text{H}}=S_{\text{H}}(0)+\frac{1}{\Gamma(\psi)}\int_{0}^{t}(t-\tau)^{\psi-1}K(\tau,\bar{S}_{\text{H}}(\tau))d\tau.$$

Integrating the inequalities in Definition 6 we get

$$\begin{aligned}\left|S_{\text{H}}-S_{\text{H}}(0)-\frac{1}{\Gamma(\psi)}\int_{0}^{t}(t-\tau)^{\psi-1}K(\tau,S_{h}(\tau))d\tau\right| &\leq \frac{1}{\Gamma(\psi)}\int_{0}^{t}(t-\tau)^{\psi-1}\Omega(\tau)d\tau\\ &\leq \frac{\epsilon\Omega(t)\Gamma(1-\psi)\sin(\pi\psi)}{\pi}.\end{aligned}\tag{27}$$

Using (27) and the Lemma we get

$$\begin{aligned}\left|S_{\text{H}}-\bar{S}_{\text{H}}\right| &\leq \left|S_{\text{H}}-\left(S_{\text{H}}(0)+\frac{1}{\Gamma(\psi)}\int_{0}^{t}(t-\tau)^{\psi-1}K(\tau,\bar{S}_{\text{H}}(\tau))d\tau\right)\right|\\ &\leq \left|S_{\text{H}}-S_{\text{H}}(0)-\left(\frac{1}{\Gamma(\psi)}\int_{0}^{t}(t-\tau)^{\psi-1}K(\tau,\bar{S}_{\text{H}}(\tau))d\tau+\frac{1}{\Gamma(\psi)}\int_{0}^{t}(t-\tau)^{\psi-1}K(\tau,S_{\text{H}}(\tau))d\tau\right.\right.\\ &- \left.\left.\frac{1}{\Gamma(\psi)}\int_{0}^{t}(t-\tau)^{\psi-1}K(\tau,S_{\text{H}}(\tau))d\tau\right)\right|\\ &\leq \left|S_{\text{H}}-S_{h}(0)-\frac{1}{\Gamma(\psi)}\int_{0}^{t}(t-\tau)^{\psi-1}K(\tau,S_{\text{H}}(\tau))d\tau\right|\\ &+ \frac{1}{\Gamma(\psi)}\int_{0}^{t}(t-\tau)^{\psi-1}\left|K(\tau,S_{h}(\tau))-K(\tau,\bar{S}_{h}(\tau))\right|d\tau\\ &\leq \frac{\epsilon\Omega(t)\Gamma(1-\psi)\sin(\pi\psi)}{\pi}+\frac{L_{\text{K}}\Gamma(1-\psi)\sin(\pi\psi)}{\pi}\int_{0}^{t}(t-\tau)^{\psi-1}\left|S_{\text{H}}(\tau)-\bar{S}_{\text{H}}(\tau)\right|d\tau\\ &\leq \frac{\epsilon\Omega(t)\Gamma(1-\psi)\sin(\pi\psi)}{\pi}E_{\psi}\left(L_{\text{KT}}^{\psi}\right).\end{aligned}$$

By setting $\kappa_\psi = \frac{\epsilon\Gamma(1-\psi)\sin(\pi\psi)}{\pi} E_\psi\left(L_{KT}^{\psi}\right)$, we have

$$\left|S_{H} - \bar{S}_{H}\right| \leq \kappa_\psi \Omega(t), \quad t \in [0, b].$$

Applying the similar approach we get

$$\left|V_{HM} - \bar{V}_{HM}\right| \leq \kappa_\psi \Omega(t), \ \left|I_{HM} - \bar{I}_{HM}\right| \leq \kappa_\psi \Omega(t),$$

$$\left|R_{HM}(t) - \bar{R}_{HM}(t)\right| \leq \kappa_\psi \Omega(t), \ \left|I_{HC}(t) - \bar{I}_{HC}(t)\right| \leq \kappa_\psi \Omega(t),$$

$$\left|R_{HC}(t) - \bar{R}_{HC}(t)\right| \leq \kappa_\psi \Omega(t), \ \left|I_{MC}(t) - \bar{I}_{MC}(t)\right| \leq \kappa_\psi \Omega(t),$$

$$\left|S_{V}(t) - \bar{S}_{V}(t)\right| \leq \kappa_\psi \Omega(t), \ \left|I_{VM}(t) - \bar{I}_{VM}(t)\right| \leq \kappa_\psi \Omega(t),$$

for every $t \in [0, b]$. Hence, we conclude that the fractional model is generalized Ulam-Hyers-Rassias stable with respect to $\Omega(t)$.

4 Numerical scheme and simulations

We carried out some numerical simulations to further explain the analytical results we presented earlier. Most of our parameters are obtained from previous works of renowned authors who have done similar works like this. However, there are few cases where certain parameters are unavailable in the literature, such cases gave us room to assume relevant values for the sake of this study.

The fractional predictor-corrector method was used in carrying out numerical simulations and the numerical scheme was derived using the Adams-Bashforth linear multi-step method in the Caputo sense, taking into consideration the convergence of the numerical method. The model is simulated using parameters provided based on dynamical data relevant to COVID-19 and Malaria co-infection in Nigeria. The total human population of Nigeria is estimated to be 206,139,587 as of 2020 and its life expectancy is estimated at 54.69 years according to WHO, hence the natural death rate ϱ_{H} is set at $\frac{1}{54.69\times365}$ per day and the recruitment rate Λ_{H} set at $\frac{206{,}139{,}597}{54.69\times365}$ per day. Under normal biological interpretation, we let all parameters used to be non-negative and considered the following initial conditions; we assume that the total susceptible population is $S_{H}(0) = 200,000,000$ and the total human population vaccinated against COVID-19, $V_{HC}(0) = 8,000,000$. Hence we set $I_{HM}(0) = 700,000, R_{HM}(0) = 100,000, I_{HC}(0) = 77,239, R_{HC}(0) = 72,350, I_{MC}(0) = 200,000$. We also assume susceptible vector population $S_{V}(0) = 50,000, I_{VM}(0) = 40,000$. It is important to state that very scanty data is available in the literature on the co-infection of COVID-19 and Malaria as of October 2021.

Let the uniform grid points be $t_k = kh$, where $k = 0, 1, 2, \ldots, m$ with some integer m and the grid step size $h = T/m$. Then by piece-wise interpolation with nodes and knots taken at t_j, $j = 0, 1, 2, \ldots, k+1$, Eq. (17) becomes the fractional variant of the one-step Adam-Moulton method (Corrector formula);

$$
\begin{aligned}
S_{\text{н}}(t_{k+1}) - S_{\text{н}}(0) &= \frac{h^{\omega}}{\Gamma(\omega+2)}\left(\sum_{j=0}^{k} u_{j,k+1} K\left(t_j, S_{\text{н}}(t_j)\right) + K\left(t_{k+1}, S_{\text{н}}^{p}(t_{k+1})\right)\right),\\
V_{\text{нс}}(t_{k+1}) - V_{\text{нс}}(0) &= \frac{h^{\omega}}{\Gamma(\omega+2)}\left(\sum_{j=0}^{k} u_{j,k+1} Q\left(t_j, V_{\text{нс}}(t_j)\right) + Q\left(t_{k+1}, V_{\text{нс}}^{p}(t_{k+1})\right)\right),\\
I_{\text{нм}}(t_{k+1}) - I_{\text{нм}}(0) &= \frac{h^{\omega}}{\Gamma(\omega+2)}\left(\sum_{j=0}^{k} u_{j,k+1} V\left(t_j, I_{\text{нм}}(t_j)\right) + H\left(t_{k+1}, I_{\text{нм}}^{p}(t_{k+1})\right)\right),\\
R_{\text{нм}}(t_{k+1}) - R_{\text{нм}}(0) &= \frac{h^{\omega}}{\Gamma(\omega+2)}\left(\sum_{j=0}^{k} u_{j,k+1} F\left(t_j, R_{\text{нм}}(t_j)\right) + K\left(t_{k+1}, R_{\text{нм}}^{p}(t_{k+1})\right)\right),\\
I_{\text{нс}}(t_{k+1}) - I_{\text{нс}}(0) &= \frac{h^{\omega}}{\Gamma(\omega+2)}\left(\sum_{j=0}^{k} u_{j,k+1} H\left(t_j, I_{\text{нс}}(t_j)\right) + Q\left(t_{k+1}, I_{\text{нс}}^{p}(t_{k+1})\right)\right),\\
R_{\text{нс}}(t_{k+1}) - R_{\text{нс}}(0) &= \frac{h^{\omega}}{\Gamma(\omega+2)}\left(\sum_{j=0}^{k} u_{j,k+1} G\left(t_j, R_{\text{нс}}(t_j)\right) + U\left(t_{k+1}, R_{\text{нс}}^{p}(t_{k+1})\right)\right),\\
I_{\text{мс}}(t_{k+1}) - I_{\text{мс}}(0) &= \frac{h^{\omega}}{\Gamma(\omega+2)}\left(\sum_{j=0}^{k} u_{j,k+1} U\left(t_j, I_{\text{мс}}(t_j)\right) + V\left(t_{k+1}, I_{\text{мс}}^{p}(t_{k+1})\right)\right),\\
S_{v}(t_{k+1}) - S_{v}(0) &= \frac{h^{\omega}}{\Gamma(\omega+2)}\left(\sum_{j=0}^{k} u_{j,k+1} P\left(t_j, S_{\text{v}}(t_j)\right) + W\left(t_{k+1}, S_{\text{v}}^{p}(t_{k+1})\right)\right),\\
I_{\text{vм}}(t_{k+1}) - I_{\text{vм}}(0) &= \frac{h^{\omega}}{\Gamma(\omega+2)}\left(\sum_{j=0}^{k} u_{j,k+1} W\left(t_j, I_{\text{vм}}(t_j)\right) + V\left(t_{k+1}, I_{\text{vм}}^{p}(t_{k+1})\right)\right),
\end{aligned}
\tag{28}
$$

where the weight

$$
u_{j,k+1} = \begin{cases} k^{\omega+1} - (k-\omega)(k+1)^{\omega}, & j = 0,\\ (k-j+2)^{\omega+1} + (k-j)^{\omega+1} - 2(k-j+1)^{\omega+1}, & 1 \le j \le k,\\ 1, & j = k+1. \end{cases}
$$

From the one-step Adams-Bashforth method, the predictor formula is presented as

$$
\begin{aligned}
S_{\text{н}}^{p}(t_{k+1}) - S_{\text{н}}(0) &= \frac{1}{\Gamma(\omega)}\sum_{j=0}^{k} v_{j,k+1} K\left(t_j, S_{\text{н}}(t_j)\right),\\
V_{\text{нс}}^{p}(t_{k+1}) - V_{\text{нс}}(0) &= \frac{1}{\Gamma(\omega)}\sum_{j=0}^{k} v_{j,k+1} Q\left(t_j, V_{\text{нс}}(t_j)\right),\\
I_{\text{нм}}^{p}(t_{k+1}) - I_{\text{нм}}(0) &= \frac{1}{\Gamma(\omega)}\sum_{j=0}^{k} v_{j,k+1} V\left(t_j, I_{\text{нм}}(t_j)\right),
\end{aligned}
$$

$$
\begin{aligned}
R^{p}_{\text{HM}}(t_{k+1}) - R_{\text{HM}}(0) &= \frac{1}{\Gamma(\omega)} \sum_{j=0}^{k} v_{j,k+1} F\left(t_j, R_{\text{HM}}(t_j)\right), \\
I^{p}_{\text{HC}}(t_{k+1}) - I_{\text{HC}}(0) &= \frac{1}{\Gamma(\omega)} \sum_{j=0}^{k} v_{j,k+1} H\left(t_j, I_{\text{HC}}(t_j)\right), \\
R^{p}_{\text{HC}}(t_{k+1}) - R_{\text{HC}}(0) &= \frac{1}{\Gamma(\omega)} \sum_{j=0}^{k} v_{j,k+1} G\left(t_j, R_{\text{HC}}(t_j)\right), \\
I^{p}_{\text{MC}}(t_{k+1}) - I_{\text{MC}}(0) &= \frac{1}{\Gamma(\omega)} \sum_{j=0}^{k} v_{j,k+1} U\left(t_j, I_{\text{MC}}(t_j)\right), \\
S^{p}_{v}(t_{k+1}) - S_{v}(0) &= \frac{1}{\Gamma(\omega)} \sum_{j=0}^{k} v_{j,k+1} P\left(t_j, S_{v}(t_j)\right), \\
I^{p}_{\text{VM}}(t_{k+1}) - I_{\text{VM}}(0) &= \frac{1}{\Gamma(\omega)} \sum_{j=0}^{k} v_{j,k+1} W\left(t_j, I_{\text{VM}}(t_j)\right),
\end{aligned}
\tag{29}
$$

where the weight

$$v_{j,k+1} = \omega^{-1} h^{\omega} \left((k-j+1)^{\omega} - (k-j)^{\omega}\right).$$

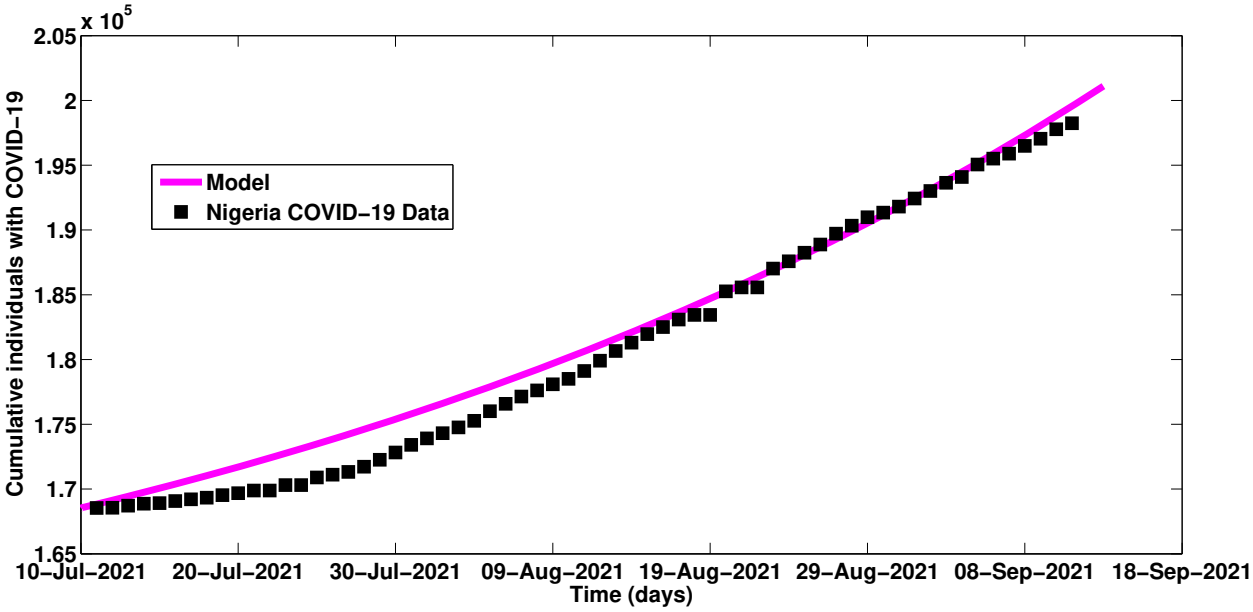

Figure 2. Fitting the cumulative number of COVID-19 reported cases

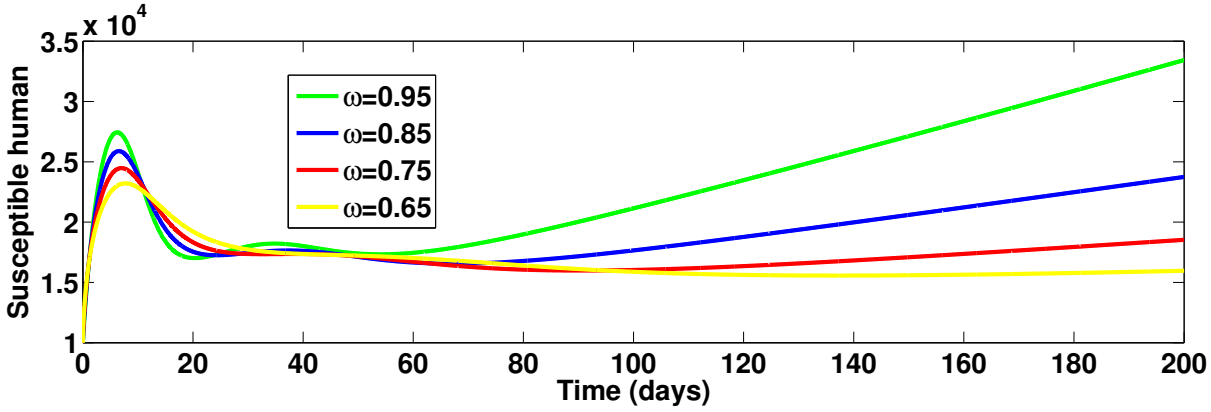

Figure 3. Simulation for susceptible human at different fractional order values

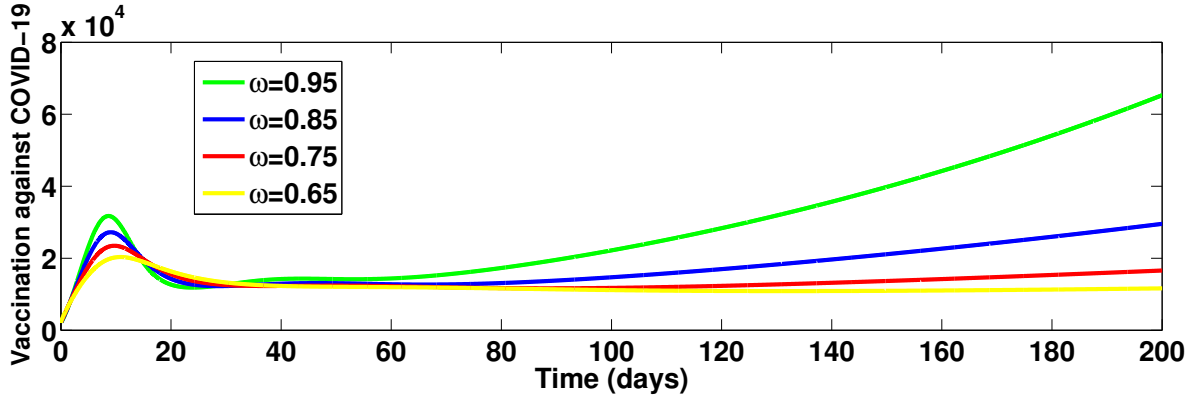

Figure 4. Simulation for vaccinated individuals against COVID-19 at different fractional order values

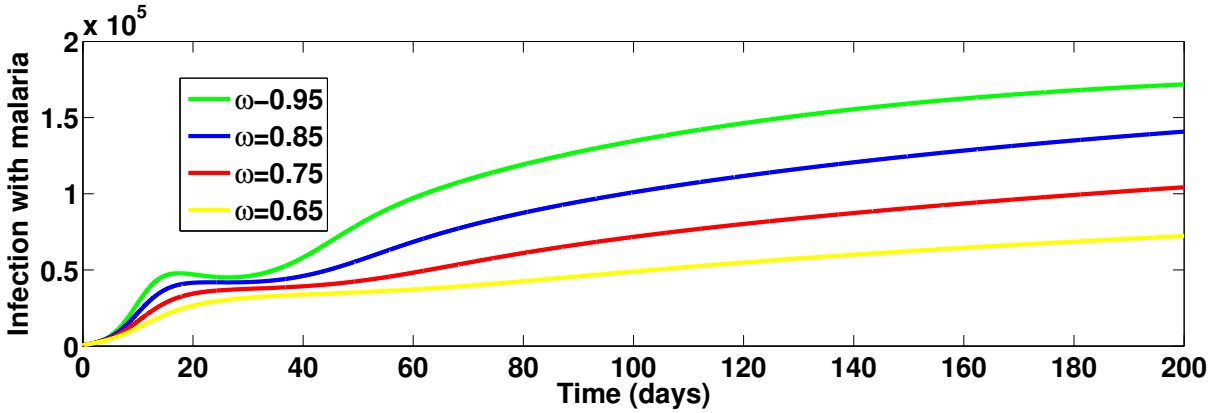

Figure 5. Simulation for individuals infected with malaria at different fractional order values

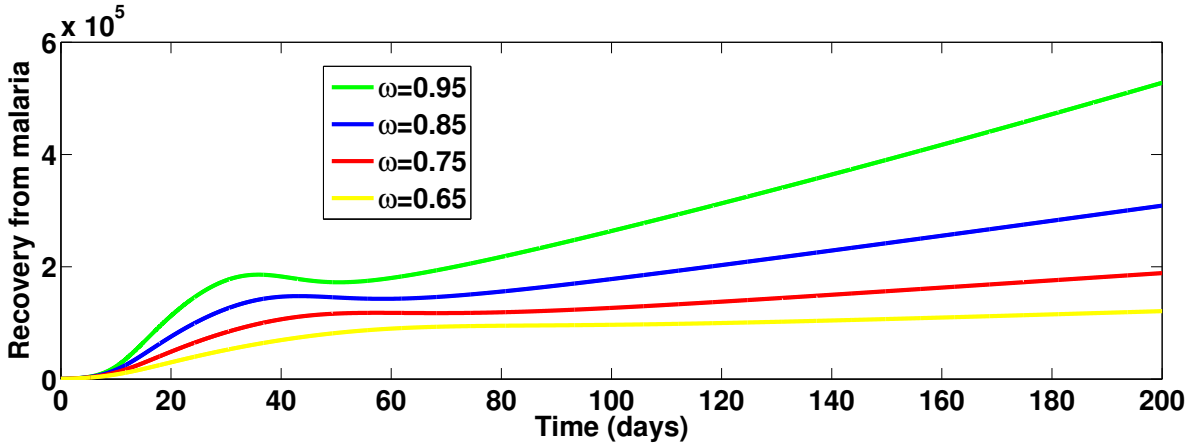

Figure 6. Simulation for individuals who recovered from malaria at different fractional order values

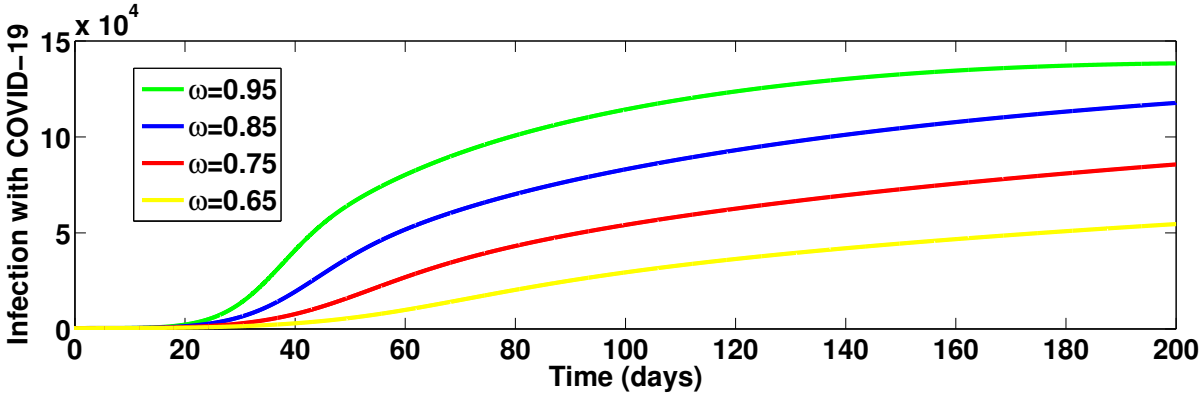

Figure 7. Simulation for individuals infected with COVID-19 at different fractional order values

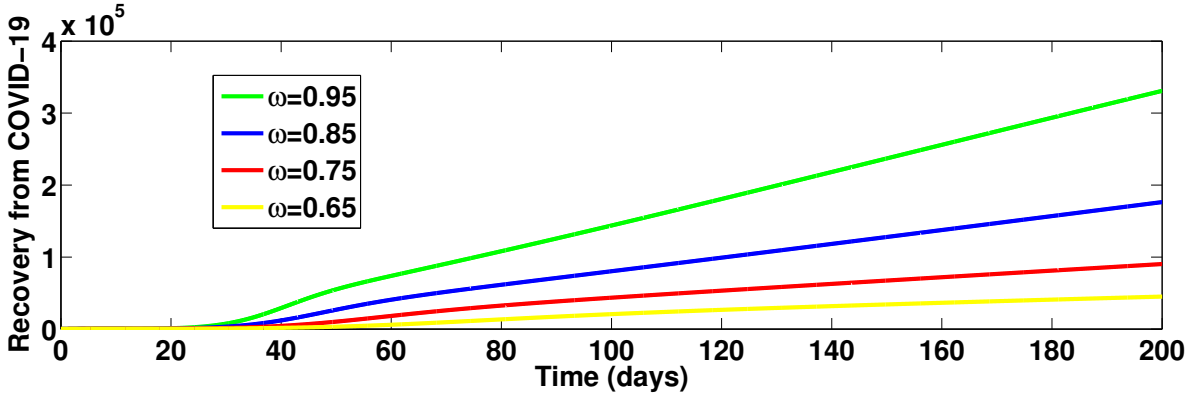

Figure 8. Simulation for individuals who recovered from COVID-19 at different fractional order values

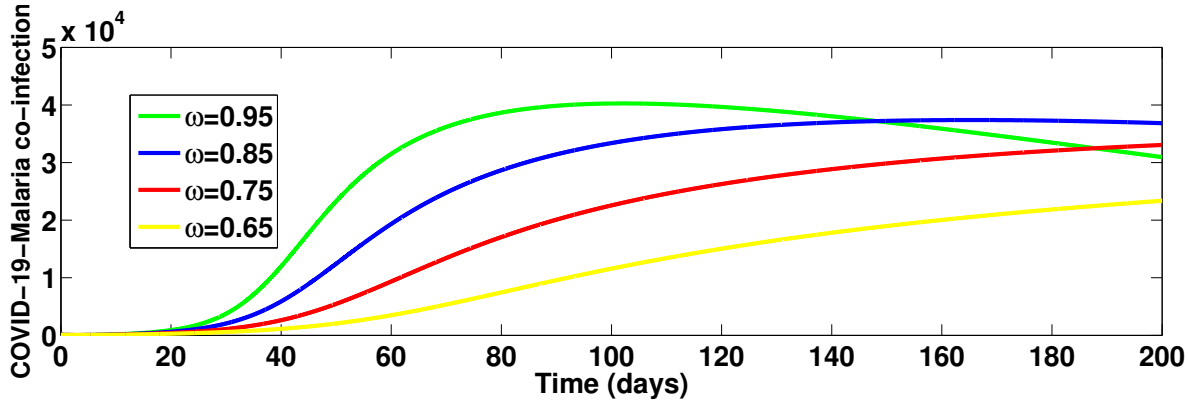

Figure 9. Simulation for individuals co-infected with COVID-19 and Malaria at different fractional order values

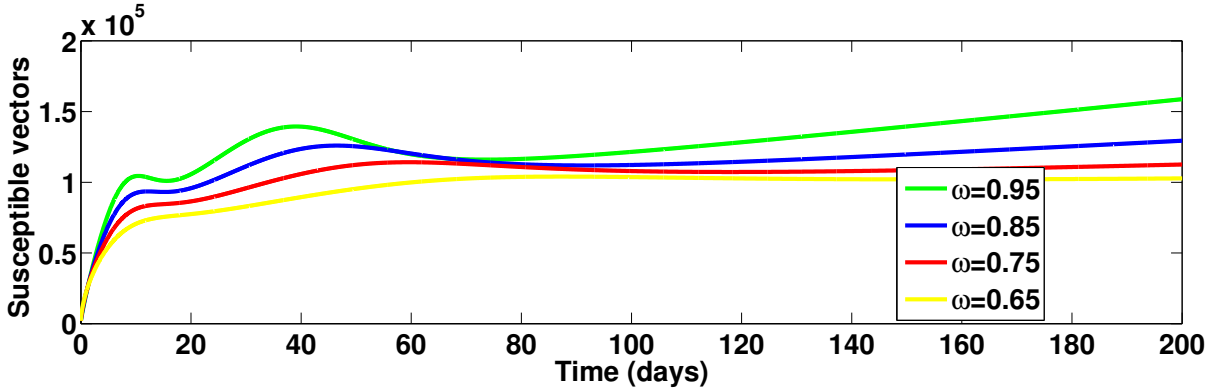

Figure 10. Simulation for susceptible vectors at different fractional order values

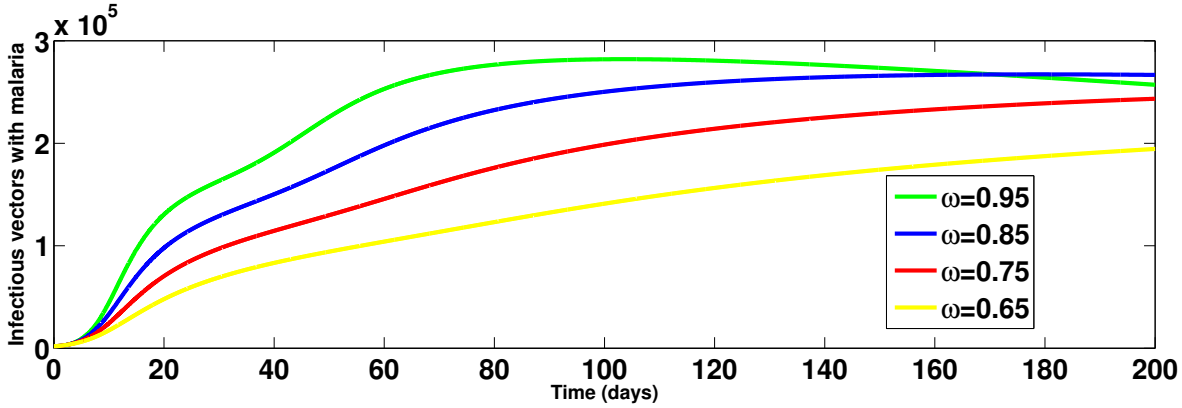

Figure 11. Simulation for infectious vectors with malaria at different fractional order values

Discussion of results

Figure 1 is the model flow diagram showing migration from one compartment to the other. Fitting of our model is presented in Figure 2 where the cumulative reported cases were used to fit the model to data from Nigeria. The figure showed that the co-infection model fits well with the Nigerian COVID-19 data for daily cumulative reported cases.

The various simulations carried out on each compartment produce distinct results of the epidemic as illustrated in the behavior of the figures. Figure 3, Figure 4, Figure 5, Figure 6, Figure 7, Figure 8, Figure 9, Figure 10 and Figure 11 are results of the compartments generated at different fractional order, $\omega = 0.95, 0.85, 0.75$ and 0.65 using parameters values from Table 1. In Figure 3, we plot the total susceptible population over time at different fractional order. It is observed that for the first 17 days, the fractional order is directly proportional to the total population; increasing the fractional order causes an increase in the susceptible population, and decreasing the fractional order reduces the population, indicating the absence of disease in the population. Between the 18th and 79th days, we experience a rapid swap in the behaviour which demonstrates the susceptibility of the human population. Figure 4 presents the simulations of individuals vaccinated against COVID-19 over time in different fractional order. It is observed that as we increase the fractional order, the number of individuals vaccinated against COVID-19 increases for the first 17 days, after which we observe a stable behaviour in the next 22 days due to the effect of vaccination on the population class. Figure 5 shows the total infectious individuals with malaria over time at different fractional order. It is observed that malaria infection causes a rapid increase in the population as fractional order increases from day one. We plot the number of individuals who have recovered from malaria over time at different fractional order in Figure 6. There is a migration from the infections class to the recovered class as shown in the population of individuals from the first day. Figure 7 presents the simulations of infectious individuals with COVID-19 over time. It is observed that fractional order has no effect on individuals with COVID-19 for the first 23 days. After 23 days, an increase in the fractional derivative order leads to an increase in the number of infectious individuals with COVID-19 and a decrease in the fractional order decreases the number of infectious individuals with COVID-19, too.

It is not until after the first 25 days that we noticed an effect due to fractional order on the number of individuals who have recovered from COVID-19 as presented in Figure 8 Accordingly, an increase in the fractional order causes an increase in the number of individuals who have recovered from COVID-19 and a decrease in the fractional directly decreases the number of individuals who have recovered from COVID-19. In Figure 9 we present the simulation of infectious individuals co-infected with malaria and COVID-19 over time in different fractional order. It is observed that the infectious population co-infected with malaria and COVID-19 is directly proportional to the fractional order after the first 24 days; an increase in the fractional order causes an increase in the co-infectious population and a decrease in population implies a decrease in the fractional order too. Figure 10 presents the simulations of susceptible vectors over time. It is observed that an increase in fractional order causes a sharp increase in the susceptible vectors and a decrease in the population of vectors implies a decrease in fractional order. In Figure 11, we plot infectious vectors with malaria over time at different fractional order. It noticed that an increase in the fractional order increases the infectious vectors with malaria and decreasing the fractional order reduces the number of infectious vectors with malaria.

Discussion of results on simulations of modification parameter on co-infection

Figure 12 presents simulations of the total co-infection class at different modification rates d_1 of $0.5, 1.0, 1.5$, and 2.0 of susceptibility of malaria-infected individuals to COVID-19 over time. It has

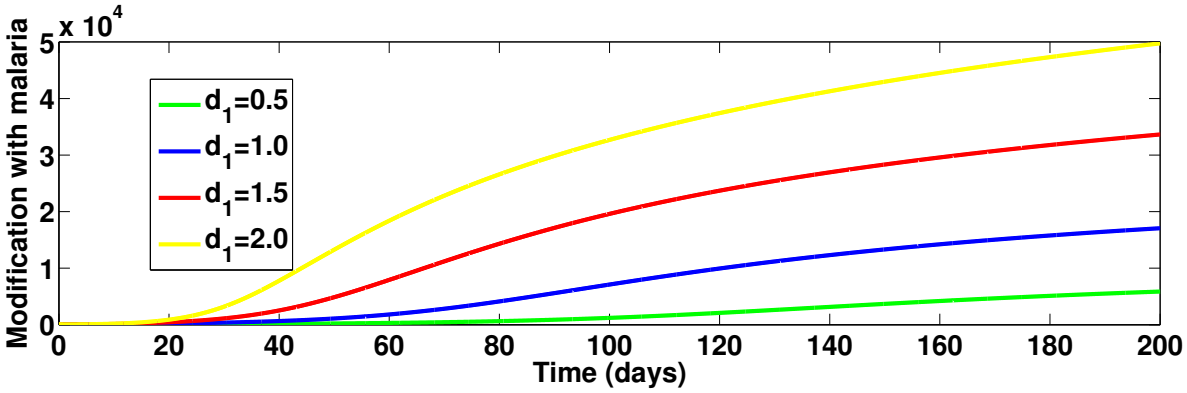

Figure 12. Modification parameter for malaria on co-infection class at different values

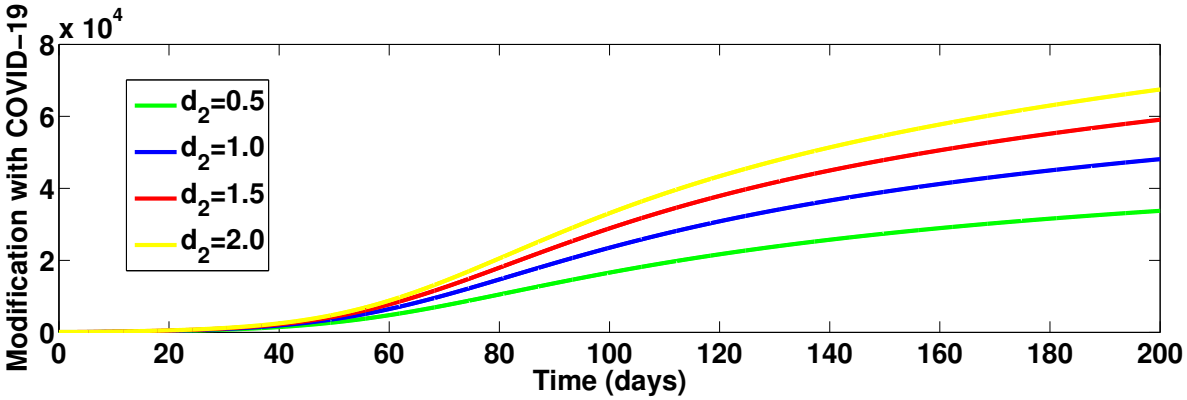

Figure 13. Modification parameter for COVID-19 on co-infection class at different values

clearly shown that, the co-infection class increases among those already infected with malaria as time increases. A clear indication that a single infection with malaria does not guarantee immunity to COVID-19. In Figure 13 we plot the simulations of the total co-infection class at different modification rates d_2 of 0.5, 1.0, 1.5, and 2.0 of susceptibility of COVID-19-infection to malaria over time. The result shows clearly that the co-infection class increases among those already infected with COVID-19. Singly infection with COVID-19 does not guarantee immunity to malaria, thereby allowing co-infection.

5 Conclusion

In this paper, we have developed a novel mathematical model for COVID-19 and Malaria and analyzed using fractional derivatives. In the results, we have shown how control measures such as vaccination and other preventive measures for either disease could help to curtail the co-infection of both diseases under an endemic scenario. The mathematical analysis of the model such as the positivity and boundedness of the equilibrium of solutions are also proven with the help of Laplace transform. We computed the basic reproduction number $\mathcal{R}_0$ and found that the COVID-19-malaria model is locally asymptotically stable when $\mathcal{R}_0 < 1$. The fractional model fits well to Nigeria's situation after fitting the model to data related to the dynamics of the co-infection disease in Nigeria. To further explain our earlier results, we simulated the model numerically and obtained several graphical results. Results of the simulation showed a good agreement between theoretical and numerical results; fractional order ω has effects on all the compartments over time and the co-infection class indicates that a single infection with malaria does not guarantee immunity to COVID-19 and infection with COVID-19 alone does not also guarantee immunity to malaria. A careful look at the findings in this work will give a better understanding of COVID-19 pandemic

and how it can be managed alongside malaria.
Based on our findings, there is a need for more awareness of the dangers of the widespread COVID-19 and the continual adherence to safety measures of malaria despite the COVID-19 lockdown. The use of face masks, maintaining social distance in gatherings, routine washing of hands, minimal travels, awareness programs, and timely hospitalization of infected individuals with mild and severe cases among other safety measures put in place to control the spread of COVID-19 need to be encouraged. For malaria cases, the use of insecticide-treated bed nets, protecting doors and windows with nets, clearing of stagnant water, drainages and bushes to avoid nurturing mosquitoes, and other routine malaria prevention strategies should be continued despite subsequent COVID-19 lock-down or restrictions. This step will go a long way in checking co-infection. The results obtained from the different simulations also explain more accurately, the various methods of prevention of infection from the two diseases. In future research, we recommend that researchers investigate the Hopf bifurcation of the delayed fractional-order COVID-19 model. See the papers [71–73] for more information.

Declarations

Use of AI tools

The authors declare that they have not used Artificial Intelligence (AI) tools in the creation of this article.

Data availability statement

All data generated or analyzed during this study are included in this article.

Ethical approval

The authors state that this research complies with ethical standards. This research does not involve either human participants or animals.

Consent for publication

Not applicable

Conflicts of interest

The authors declare that they have no conflict of interest.

Funding

Not applicable

Author's contributions

L.L.I.: Conceptualization, Formal Analysis, Software, Validation, Data Curation, Writing-Original Draft. A.O.: Methodology, Supervision and Editing. S.C.I.: Supervision and Review. The authors have read and agreed to the published version of the manuscript.

Acknowledgements

Not applicable

References

[1] Cowman, A.F., Healer, J., Marapana, D. and Marsh, K. Malaria: biology and disease. *Cell*, 167(3), 610-624, (2016). [CrossRef]

[2] Centers for Disease Control and Prevention (CDC), The History of Malaria, an Ancient Disease, (2018). https://stacks.cdc.gov/view/cdc/135582

[3] Mandal, S., Sarkar, R.R. and Sinha, S. Mathematical models of Malaria-a review. *Malaria Journal*, 10, 202, (2011). [CrossRef]

[4] World Health Organization (WHO), World Malaria Report 2015, (2015). https://iris.who.int/handle/10665/200018, https://www.pmi.gov/press-release-world-malaria-report-2015-released-today

[5] World Health Organization (WHO), Malaria key facts, (2023). https://www.who.int/news-room/fact-sheets/detail/malaria

[6] World Health Organization (WHO), Malaria, (2021). https://www.afro.who.int/health-topics/malaria

[7] World Health Organization (WHO), World Malaria Report 2019, (2019). https://www.who.int/publications/i/item/9789241565721

[8] Nigeria Malaria Indicator Survey (MIS) 2015, pp.96-99, (2015). https://dhsprogram.com/pubs/pdf/mis20/mis20.pdf

[9] USAID, U.S. President's Malaria Initiative Nigeria Malaria Operational Plan FY 2020, (2020). https://d1u4sg1s9ptc4z.cloudfront.net/uploads/2021/03/fy-2020-nigeria-malaria-operational-plan.pdf

[10] Abdu, E.M. and Mariamenatu, A.H. Biological property of novel coronavirus SARS-CoV-2 (2019-nCoV). *International Journal of Applied Sciences and Biotechnology*, 9(1), 16-22, (2021). [CrossRef]

[11] Mohan, B.S. and Nambier, V. COVID-19: an insight into SARS-CoV-2 pandemic originated at Wuhan City in Hubei Province of China. *Infectious Diseases and Epidemiology*, 6(4), 146, (2020). [CrossRef]

[12] Salahshoori, I., Mobaraki-Asl, N., Seyfaee, A., Mirzaei Nasirabad, N., Dehghan, Z., Faraji, M. et al. Overview of COVID-19 disease: virology, epidemiology, prevention diagnosis, treatment, and vaccines. *Biologics*, 1(1), 2-40, (2021). [CrossRef]

[13] Adhikari, S.P., Meng, S., Wu, Y.J., Mao, Y.P., Ye, R.X., Wang, Q.Z. et al. Epidemiology, causes, clinical manifestation and diagnosis, prevention and control of coronavirus disease (COVID-19) during the early outbreak period: a scoping review. *Infectious Diseases of Poverty*, 9, 29, (2020). [CrossRef]

[14] United States Food and Drug Administration: FDA Briefing Document. Pfizer-BioNTech COVID-19 vaccine, (2020). https://www.fda.gov/media/144245/download

[15] Park, M., Cook, A.R., Lim, J.T., Sun, Y. and Dickens, B.L. A systematic review of COVID-19 epidemiology based on current evidence. *Journal of Clinical Medicine*, 9(4), 967, (2020). [CrossRef]

[16] WHO, Corona Virus Disease 2019 (COVID-19) Situation Report-97. Surveillance, (2020). https://www.who.int/docs/default-source/coronaviruse/situation-reports/20200426-sitrep-97-covid-19.pdf

[17] World Health Organization (WHO), WHO COVID-19 Dashboard, (2024). https://data.who.

int/dashboards/covid19/cases

[18] Reliefweb, World Malaria Report 2021, (2021). https://reliefweb.int/report/world/world-malaria-report-2021

[19] Hussain, S., Madi, E.N., Khan, H., Gulzar, H., Etemad, S., Rezapour, S. et al. On the stochastic modeling of COVID-19 under the environmental white noise. *Journal of Function Spaces,* 2022, 4320865, (2022). [CrossRef]

[20] Ahmed, K.M., Haroun, M.S.E.H., Hussien, A. and Omer, M.E.A. COVID-19 and Malaria Co-infection; same coin but different faces?. *Available at SSRN,* (2021). [CrossRef]

[21] Boukhouima, A., Lotfi, E.M., Mahrouf, M., Rosa, S., Torres, D.F. and Yousfi, N. Stability analysis and optimal control of a fractional HIV-AIDS epidemic model with memory and general incidence rate. *The European Physical Journal Plus,* 136, 103, (2021). [CrossRef]

[22] Traoré, B., Sangaré, B. and Traoré, S. A mathematical model of Malaria transmission with structured vector population and seasonality. *Journal of Applied Mathematics,* 2017, 6754097, (2017). [CrossRef]

[23] Chiyaka, C., Tchuenche, J.M., Garira, W. and Dube, S. A mathematical analysis of the effects of control strategies on the transmission dynamics of malaria. *Applied Mathematics and Computation,* 195(2), 641-662, (2008). [CrossRef]

[24] Macdonald, G. *The Epidemiology and Control of Malaria.* Oxford University Press: London, UK, (1957).

[25] Egeonu, K.U., Omame, A. and Inyama, S.C. A co-infection model for two-strain malaria and cholera with optimal control. *International Journal of Dynamics and Control,* 9, 1612-1632, (2021). [CrossRef]

[26] Ross, R. *The Prevention of Malaria.* John Murray: London, UK, (1911).

[27] Tchoumi, S.Y., Diagne, M.L., Rwezaura, H. and Tchuenche, J.M. Malaria and COVID-19 co-dynamics: A mathematical model and optimal control. *Applied Mathematical Modelling,* 99, 294-327, (2021). [CrossRef]

[28] Musa, S.S., Qureshi, S., Zhao, S., Yusuf, A., Mustapha, U.T. and He, D. Mathematical modeling of COVID-19 epidemic with effect of awareness programs. *Infectious Disease Modelling,* 6, 448-460, (2021). [CrossRef]

[29] Daniel, D.O. Mathematical model for the transmission of COVID-19 with nonlinear forces of infection and the need for prevention measure in Nigeria. *Journal of Infectious Diseases and Epidemiology,* 6(5), 158, (2020). [CrossRef]

[30] Omame, A., Nnanna, C.U. and Inyama, S.C. Optimal control and cost-effectiveness analysis of an HPV–Chlamydia trachomatis co-infection model. *Acta Biotheoretica,* 69, 185-223, (2021). [CrossRef]

[31] Omame, A. and Okuonghae, D. A co-infection model for oncogenic Human papillomavirus and tuberculosis with optimal control and cost-effectiveness analysis. *Optimal Control Applications and Methods,* 42(4), 1081-1101, (2021). [CrossRef]

[32] Mtisi, E., Rwezaura, H. and Tchuenche, J.M. A mathematical analysis of malaria and tuberculosis co-dynamics. *Discrete and Continuous Dynamical Systems-B,* 12(4), 827-864, (2009). [CrossRef]

[33] Iwa, L.L., Nwajeri, U.K., Atede, A.O., Panle, A.B. and Egeonu, K.U. Malaria and cholera co-dynamic model analysis furnished with fractional-order differential equations. *Mathematical*

Modelling and Numerical Simulation with Applications, 3(1), 33-57, (2023). [CrossRef]

[34] Thabet, S.T.M., Abdo, M.S. and Shah, K. Theoretical and numerical analysis for transmission dynamics of COVID-19 mathematical model involving Caputo–Fabrizio derivative. *Advances in Difference Equations*, 2021, 184, (2021). [CrossRef]

[35] Uçar, E., Uçar, S., Evirgen, F. and Özdemir, N. A fractional SAIDR model in the frame of Atangana–Baleanu derivative. *Fractal and Fractional*, 5(2), 32, (2021). [CrossRef]

[36] Mohammadi, H., Kumar, S., Rezapour, S. and Etemad, S. A theoretical study of the Caputo–Fabrizio fractional modeling for hearing loss due to Mumps virus with optimal control. *Chaos, Solitons & Fractals*, 144, 110668, (2021). [CrossRef]

[37] Najafi, H., Etemad, S., Patanarapeelert, N., Asamoah, J.K.K., Rezapour, S. and Sitthiwirattham, T. A study on dynamics of CD4$^+$ T-cells under the effect of HIV-1 infection based on a mathematical fractal-fractional model via the Adams-Bashforth scheme and Newton polynomials. *Mathematics*, 10(9), 1366, (2022). [CrossRef]

[38] Batiha, I.M., Momani, S., Ouannas, A., Momani, Z. and Hadid, S.B. Fractional-order COVID-19 pandemic outbreak: Modeling and stability analysis. *International Journal of Biomathematics*, 15(01), 2150090, (2022). [CrossRef]

[39] Badshah, N. and Akbar, H. Stability analysis of fractional order SEIR model for malaria disease in Khyber Pakhtunkhwa. *Demonstratio Mathematica*, 54(1), 326-334, (2021). [CrossRef]

[40] Uçar, S. Analysis of hepatitis B disease with fractal–fractional Caputo derivative using real data from Turkey. *Journal of Computational and Applied Mathematics*, 419, 114692, (2023). [CrossRef]

[41] Nwajeri, U.K., Panle, A.B., Omame, A., Obi, M.C. and Onyenegecha, C.P. On the fractional order model for HPV and Syphilis using non–singular kernel. *Results in Physics*, 37, 105463, (2022). [CrossRef]

[42] Rezapour, S., Etemad, S. and Mohammadi, H. A mathematical analysis of a system of Caputo–Fabrizio fractional differential equations for the anthrax disease model in animals. *Advances in Difference Equations*, 2020, 481, (2020). [CrossRef]

[43] Matar, M.M., Abbas, M.I., Alzabut, J., Kaabar, M.K.A., Etemad, S. and Rezapour, S. Investigation of the p-Laplacian nonperiodic nonlinear boundary value problem via generalized Caputo fractional derivatives. *Advances in Difference Equations*, 2021, 68, (2021). [CrossRef]

[44] Etemad, S. and Rezapour, S. On the existence of solutions for fractional boundary value problems on the ethane graph. *Advances in Difference Equations*, 2020, 276, (2020). [CrossRef]

[45] Özköse, F. and Yavuz, M. Investigation of interactions between COVID-19 and diabetes with hereditary traits using real data: A case study in Turkey. *Computers in Biology and Medicine*, 141, 105044, (2022). [CrossRef]

[46] Agarwal, P., Ramadan, M.A., Rageh, A.A. and Hadhoud, A.R. A fractional-order mathematical model for analyzing the pandemic trend of COVID-19. *Mathematical Methods in the Applied Sciences*, 45(8), 4625-4642, (2022). [CrossRef]

[47] Wu, Y., Ahmad, S., Ullah, A. and Shah, K. Study of the fractional-order HIV-1 infection model with uncertainty in initial data. *Mathematical Problems in Engineering*, 2022, 7286460, (2022). [CrossRef]

[48] Ogunrinde, R.B., Nwajeri, U.K., Fadugba, S.E., Ogunrinde, R.R. and Oshinubi, K.I. Dynamic model of COVID-19 and citizens reaction using fractional derivative. *Alexandria Engineering Journal*, 60(2), 2001-2012, (2021). [CrossRef]

[49] Nwajeri, U.K., Omame, A. and Onyenegha, C.P. Analysis of a fractional order model for HPV and CT co-infection. *Results in Physics,* 28, 104643, (2021). [CrossRef]

[50] Ul Rehman, A., Singh, R. and Agarwal, P. Modeling, analysis and prediction of new variants of COVID-19 and dengue co-dynamics on complex networks. *Chaos, Solitons & Fractals,* 150, 111008, (2021). [CrossRef]

[51] Djenina, N., Ouannas, A., Batiha, I.M., Grassi, G., Oussaeif, T.E. and Momani, S. A novel fractional-order discrete SIR model for predicting COVID-19 behavior. *Mathematics,* 10(13), 2224, (2022). [CrossRef]

[52] Abioye, A.I., Peter, O.J., Ogunseye, H.A., Oguntolu, F.A., Ayoola, T.A. and Oladapo, A.O. A fractional-order mathematical model for malaria and COVID-19 co-infection dynamics. *Healthcare Analytics,* 4, 100210, (2023). [CrossRef]

[53] Hussein, R., Guedes, M., Ibraheim, N., Ali, M.M., El-Tahir, A., Allam, N. et al. Impact of COVID-19 and malaria coinfection on clinical outcomes: a retrospective cohort study. *Clinical Microbiology and Infection,* 28(8), 1152.e1-1152.e6, (2022). [CrossRef]

[54] Khan, M.A. and Atangana, A. Modeling the dynamics of novel coronavirus (2019-nCov) with fractional derivative. *Alexandria Engineering Journal,* 59(4), 2379-2389, (2020). [CrossRef]

[55] Gorenflo, R. and Mainardi, F. Fractional calculus. In *Fractals and Fractional Calculus in Continuum Mechanics* (Vol. 378) (pp. 223-276). Vienna, Austria: Springer, (1997). [CrossRef]

[56] Buonomo, B. Analysis of a malaria model with mosquito host choice and bed-net control. *International Journal of Biomathematics,* 8(06), 1550077, (2015). [CrossRef]

[57] Agusto, F.B. Optimal isolation control strategies and cost-effectiveness analysis of a two-strain avian influenza model. *Biosystems,* 113(3), 155-164, (2013). [CrossRef]

[58] Zio, S., Tougri, I. and Lamien, B. Propagation du COVID19 au burkina faso, modelisation bayesienne et quantification des incertitudes: premiere approche. *Ecole Polytechnique de Ouagadougou (EPO) Ouagadougou,* (2020).

[59] Our World in Data, Coronavirus (COVID-19) Vaccinations, (2022). https://ourworldindata.org/covid-vaccinations

[60] Liu, Z., Magal, P., Seydi, O. and Webb, G. A COVID-19 epidemic model with latency period. *Infectious Disease Modelling,* 5, 323-337, (2020). [CrossRef]

[61] Chitnis, N., Hyman, J.M. and Cushing, J.M. Determining important parameters in the spread of malaria through the sensitivity analysis of a mathematical model. *Bulletin of Mathematical Biology,* 70, 1272-1296, (2008). [CrossRef]

[62] Ngonghala, C.N., Iboi, E., Eikenberry, S., Scotch, M., MacIntyre, C.R., Bonds, M.H. and Gumel, A.B. Mathematical assessment of the impact of non-pharmaceutical interventions on curtailing the 2019 novel coronavirus. *Mathematical Biosciences,* 325, 108364, (2020). [CrossRef]

[63] Okuonghae, D. and Omame, A. Analysis of a mathematical model for COVID-19 population dynamics in Lagos, Nigeria. *Chaos, Solitons & Fractals,* 139, 110032, (2020). [CrossRef]

[64] Zhang, Z., Zeb, A., Egbelowo, O.F. and Erturk, V.S. Dynamics of a fractional order mathematical model for COVID-19 epidemic. *Advances in Difference Equations,* 2020, 420, (2020). [CrossRef]

[65] Van den Driessche, P. and Watmough, J. Reproduction numbers and sub-threshold endemic equilibria for compartmental models of disease transmission. *Mathematical Biosciences,* 180(1-2), 29-48, (2002). [CrossRef]

[66] Sene, N. SIR epidemic model with Mittag–Leffler fractional derivative. *Chaos, Solitons & Fractals*, 137, 109833, (2020). [CrossRef]

[67] Demirci, E. and Ozalp, N. A method for solving differential equations of fractional order. *Journal of Computational and Applied Mathematics*, 236(11), 2754-2762, (2012). [CrossRef]

[68] Diethelm, K., Ford, N.J. and Freed, A.D. A predictor-corrector approach for the numerical solution of fractional differential equations. *Nonlinear Dynamics*, 29, 3-22, (2002). [CrossRef]

[69] Lin, W. Global existence theory and chaos control of fractional differential equations. *Journal of Mathematical Analysis and Applications*, 332(1), 709-726, (2007). [CrossRef]

[70] Liu, K., Feckan, M. and Wang, J. Hyers–Ulam stability and existence of solutions to the generalized Liouville–Caputo fractional differential equations. *Symmetry*, 12(6), 955, (2020). [CrossRef]

[71] Huang, C., Wang, J., Chen, X. and Cao, J. Bifurcations in a fractional-order BAM neural network with four different delays. *Neural Networks*, 141, 344-354, (2021). [CrossRef]

[72] Xu, C., Mu, D., Liu, Z., Pang, Y., Liao, M. and Aouiti, C. New insight into bifurcation of fractional-order 4D neural networks incorporating two different time delays. *Communications in Nonlinear Science and Numerical Simulation*, 118, 107043, (2023). [CrossRef]

[73] Xu, C., Zhang, W., Aouiti, C., Liu, Z. and Yao, L. Bifurcation insight for a fractional-order stage-structured predator–prey system incorporating mixed time delays. *Mathematical Methods in the Applied Sciences*, 46(8), 9103-9118, (2023). [CrossRef]

Bulletin of Biomathematics (BBM)
(https://bulletinbiomath.org)

How to cite this article: Iwa, L.L., Omame, A. & Inyama, S.C. (2024). A fractional-order model of COVID-19 and Malaria co-infection. *Bulletin of Biomathematics*, 2(2), 133-161. https://doi.org/10.59292/bulletinbiomath.2024006